

1 Annual high-resolution grazing intensity maps on the 2 Qinghai-Tibet Plateau from 1990 to 2020

3 Jia Zhou^{1,2}, Jin Niu³, Ning Wu¹, Tao Lu^{1*}

4 ¹Chengdu Institute of Biology, Chinese Academy of Sciences, Chengdu 610213, China

5 ²University of Chinese Academy of Sciences, Beijing 100049, China

6 ³Department of Economics, Brown University, Providence, 02912, USA

7 Correspondence to: Tao Lu (lutao@cib.ac.cn)

8 **Abstract.** Grazing activities constitute the paramount challenge to grassland conservation over the
9 Qinghai-Tibet Plateau (QTP), underscoring the urgency for obtaining detailed extent, patterns, and
10 trends of grazing information to access efficient grassland management and sustainable development.
11 Here, to inform these issues, we provided the first annual Gridded Dataset of Grazing Intensity maps
12 (GDGI) with a resolution of 100 meters from 1990 to 2020 for the QTP. Five most commonly used
13 machine learning algorithms were leveraged to develop livestock spatialization model, which spatially
14 disaggregate the livestock census data at the county level into a detailed 100 m× 100 m grid, based on
15 seven key predictors from terrain, climate, vegetation and socio-economic factors. Among these
16 algorithms, the extreme trees (ET) model performed the best in representing the complex nonlinear
17 relationship between various environmental factors and livestock intensity, with an average absolute
18 error of just 0.081 SU/hm², a rate outperforming the other models by 21.58%–414.60%. By using the
19 ET model, we further generated the GDGI dataset for the QTP to reveal the spatio-temporal
20 heterogeneity and variation in grazing intensities. The GDGI indicates grazing intensity remained high
21 and largely stable from 1990 to 1997, followed by a sharp decline from 1997 to 2001, and fluctuated
22 thereafter. Encouragingly, comparing with other open-access datasets for grazing distribution on the
23 QTP, the GDGI has the highest accuracy, with the determinant coefficient (R^2) exceed 0.8. Given its
24 high resolution, recentness and robustness, we believe that the GDGI dataset can significantly enhance
25 understanding of the substantial threats to grasslands emanating from overgrazing activities.
26 Furthermore, the GDGI product holds considerable potential as a foundational source for other
27 researches, facilitating rational utilization of grasslands, refined environmental impact assessments, and
28 the sustainable development of animal husbandry. The GDGI product developed in this study is
29 available at <https://doi.org/10.5281/zenodo.13141090-1085111913672152> (Zhou et al., 2024).

30
31

带格式的：不取消行号

32 1 Introduction

33 Livestock is a crucial contributor to global food systems through the provision of essential animal
34 proteins and fats, and plays a significant role in supporting human survival and socio-economic
35 development (Gilbert et al., 2018; Godfray et al., 2018; Humpenöder et al., 2022; Kumar et al., 2022).
36 However, the escalating increase in human demand for meat and dairy products over recent decades has
37 triggered a livestock boom, which in turn has increasingly threatened grassland ecosystems and placed
38 a heavy burden on the environment through overgrazing and land-use change (Tabassum et al., 2016;
39 Wei et al., 2022; Minoofar et al., 2023). It is estimated that up to 300 million hectares of land are used
40 globally for grazing and cultivating fodder crops (Tabassum et al., 2016). Grazing activities could alter
41 vegetation phenology and community structure (Dong et al., 2020), and trigger deforestation (García
42 Ruiz et al., 2020), grassland degradation (Sun et al., 2020), soil erosion (Shakoor et al., 2021), and
43 associated direct releases in greenhouse gas that lead to climate change feedback (Godfray et al., 2018;
44 Chang et al., 2021). Additionally, livestock are responsible for large-scale dispersion of pathogens,
45 organic matter, and residual medications into soil and groundwater, thereby contaminating the
46 environment (Venglovsky et al., 2009; Tabassum et al., 2016; Hu et al., 2017; Muloi et al., 2022).
47 Consequently, more and more scholars have called attention to provide reliable contemporary dataset to
48 illustrate the spatio-temporal heterogeneity and variation of livestock (Petz et al., 2014; Fetzel et al.,
49 2017; Zhang et al., 2018; Li et al., 2021).

50 One of the major challenges in monitoring grazing activity at regional or even larger scale, is the
51 determination of the livestock distribution pattern. Despite the importance of geographical grazing
52 information, high spatio-temporal grazing dataset remain unavailable, posing the most critical challenge
53 to grassland management, particularly for vulnerable grassland ecosystems in fragile regions grappling
54 with economic and sustainable development contradictions (Meng et al., 2023; Pozo et al., 2021; Miao et
55 al., 2020; He et al., 2022). In the early 2000s, the Food and Agriculture Organization of the United
56 Nations (FAO) launched the Gridded Livestock of the World (GLW) project to facilitate a detailed
57 evaluation of livestock production, aiming to provide pixel-scale livestock densities instead of traditional
58 administrative unit benchmarks (Nicolas et al., 2016). Consequently, the world's inaugural dataset of
59 livestock spatialization map (GLW1) was released in 2007, providing the first globally standardized
60 livestock density distribution map at a spatial resolution of 0.05 decimal degrees (≈ 5 km at the equator)
61 for 2002. It was not until 2014 that an updated GLW2 map with a 1 km resolution for 2006 was
62 released, by using a stratified regression approach, superior spatial resolution predictor variables, and
63 more detailed livestock census data (Robinson et al., 2014). Furthermore, an evolutionary step in
64 machine learning technology saw Gilbert et al. (2018) using random forests algorithm to forge a global
65 livestock distribution map with a 10-km resolution for 2010 (GLW3), succeeding traditional multivariate
66 regression methods and surpassing the precision of previous GLW1 and GLW2 maps. Beyond these

67 global mappings, several maps with different scales have also been published, including intercontinental,
68 national, state or provincial, and local scale (Neumann et al., 2009; Prosser et al., 2011; Van Boeckel
69 et al., 2011; Nicolas et al., 2016). However, these maps are fundamentally coarse due to constraints such as
70 the availability of fine scale and contemporary census data, the grazing spatialization method, as well as
71 the identification of appropriate indicators, thereby limiting their application to local or regional-scale
72 studies (Nicolas et al., 2016; Gilbert et al., 2018; Robinson et al., 2014). Hence, there is an emergent
73 demand for more refined grazing map products (Mulligan et al., 2020; Martinuzzi et al., 2021).

74 An exemplar of this need can be observed in the Qinghai-Tibet Plateau (QTP), the world's most
75 elevated pastoral region and an important grazing area in China (Zhan et al., 2023). It was possessing
76 abundant grassland that spans 1.5 million km², accounting for 50.43% of China's total grassland area,
77 with Yak and Tibetan sheep as primary grazing livestock (Feng et al., 2009; Cai et al., 2014; Zhan et al.,
78 2023). Over recent decades, the QTP has undergone escalating grassland degradation, leading to many
79 ecological and socio-economic problems, which calls for an urgent need for detailed livestock
80 distribution dataset (Li et al., 2022a). Unfortunately, despite researchers' efforts at mapping the QTP's
81 grazing intensity, current livestock dataset still suffer from coarse spatio-temporal resolution and
82 modelling accuracy. Apart from the aforementioned global grazing dataset, several other maps also
83 cover the QTP. For instance, Liu et al. (2021) generated annual 250-m gridded carrying capacity maps
84 for 2000-2019, by employing multiple linear regressions of livestock numbers, population density, NPP,
85 and topographic features. Li et al. (2021) used machine learning algorithms to produce gridded livestock
86 distribution data at 1 km resolution for 2000-2015 in western China at five year interval, based on
87 county-level livestock census data and 13 factors from land use practice, topography, climate, and
88 socioeconomic aspects, including grassland coverage, arable land coverage, forest land coverage, desert
89 coverage, NDVI, elevation, slope, daytime surface temperature, precipitation, distance to river, travel
90 time to major cities, population density, and GDP (Li et al., 2021). A contribution from Meng et al. (2023)
91 brought forth annual longer time-series grazing maps by using random forests model, integrating climate,
92 soil, NDVI, water distance, and settlement density to decompose county-level livestock census data to a
93 0.083° (≈10 km at the equator) grid for 1982-2015 (Meng et al., 2023). Similarly, Zhan et al. (2023) also
94 used random forests algorithm to combine eleven influence factors to provide a winter and summer
95 grazing density map at 500 m resolution for 2020 (Zhan et al., 2023).

96 However, although these maps have provided good help in understanding grazing conditions on the
97 QTP, there are currently still no maps that can satisfy the need for fine-scale grassland management
98 with a long time span. In addition, the available livestock distribution maps of the QTP still need
99 improvement in terms of modelling techniques and factor selection to obtain high-precision livestock
100 spatialization data. For example, traditional methods like multiple linear regression, while proven
101 fundamental and widely applicable for livestock spatialization (Robinson et al., 2014; Ma et al., 2022),
102 are being challenged by the development of computational science in recent years. Among them,
103 machine learning technology is providing new opportunities towards more accurate predictions of
104 livestock distribution (García et al., 2020). Random forests regression, for instance, is currently widely
105 used to construct global, national as well as regional livestock spatialization dataset, and has been proved
106 to have much better accuracy than traditional mapping techniques (Rokach, 2016; Nicolas et al., 2016;
107 Gilbert et al., 2018; Dara et al., 2020; Chen et al., 2019; Li et al., 2021). Nevertheless, other more
108 advanced machine learning methods with superior feature learning and more robust generalization
109 capabilities, remains largely untapped for modelling geographic data (Ahmad et al., 2018; Heddam et al.,

110 2020; Long et al., 2022). Thus, exploring the potential application of new advanced machine learning
111 technologies in livestock spatialization remains a critical task. Furthermore, selecting the suitable factors
112 that influencing livestock grazing preferences is also the other critical challenge for enhancing the
113 precision of grazing distribution dataset (Meng et al., 2023). Livestock grazing activities are often
114 affected by abiotic and biotic resources, including climatic and environmental factors (Waha et al.,
115 2018), herd foraging and grazing behaviours (Garrett et al., 2018; Miao et al., 2020), and
116 conservation-oriented policies (Li et al., 2021). For instance, regions exceeding elevations of 5,600 m or
117 slope greater than 40% are customarily unsuitable for grazing (Luo et al., 2013; Mack et al., 2013;
118 Robinson et al., 2014; Chen et al., 2019). Moreover, the livestock generally prefer areas abundant in
119 water and pasture resources for foraging (Li et al., 2021). Besides, ecological conservation policies also
120 exert substantial influence, significantly affecting grazing distribution relative to the level of
121 conservation priority. In addition, the health status of the grassland is an important factor influencing
122 whether livestock choose to feed or not (Li et al., 2021). Consequently, indicators related to the above
123 aspects are often employed to gauge the spatial heterogeneity of livestock distribution (Allred et al., 2013;
124 Sun et al., 2021; Meng et al., 2023). Nonetheless, some most commonly used indicators like NPP or
125 NDVI can result in misconceptions, as they may not fully characterize the grazing intensity. For example,
126 grasslands with high NPP or NDVI are often preferred by livestock, but this doesn't necessarily correlate
127 with grazing intensity in nature reserves due to strict policy restrictions (Veldhuis et al., 2019; O'Neill and
128 Abson, 2009; Zhang et al., 2021b). Conversely, areas with sparse grassland cover may support
129 considerable livestock numbers, despite evidence of degradation (Zhang et al., 2021a; Guo et al., 2015).
130 Accordingly, further investigation of novel indicators is imperative to enhance the correlation between
131 grassland and grazing intensity, thereby optimizing the integration of such influencing factors into
132 grazing spatialization models.

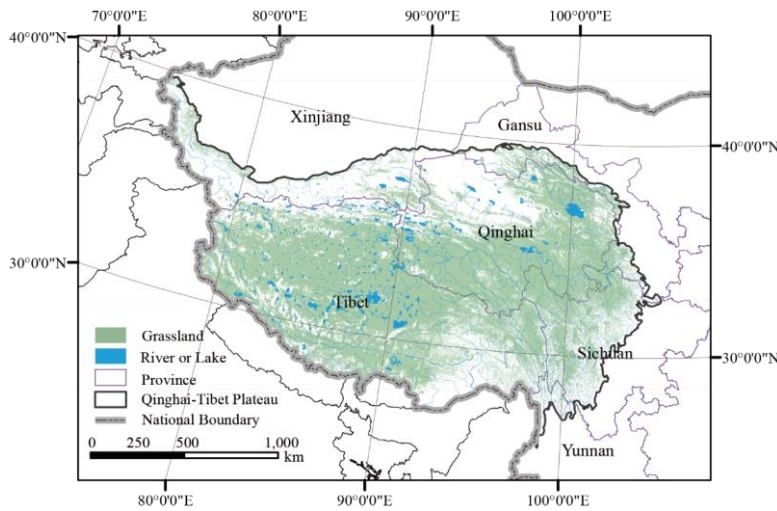
133 In summary, the QTP is in pressing need for a high spatio-temporal resolution grazing dataset to
134 address urgent and realistic challenges. But the existing livestock dataset specific to the QTP are fraught
135 with several insufficient, predominantly concerning rough resolution, relatively backward census data,
136 as well as conventional methods in livestock spatialization. Moreover, the discrepancies in predictive
137 indicators and modelling approaches within these dataset discourage their application in time-series
138 analysis. Consequently, the generation of high-resolution and high-quality grazing map products has
139 emerged as the most pressing challenge for the QTP. Here, we aim to (1) establish a methodological
140 framework by using more rational models and indicators than traditional studies to achieve fine-scale
141 livestock spatialization; (2) select the grazing spatialization model with good performance by
142 incorporating multi-source data with advanced machine learning techniques; and (3)—ultimately,
143 provide an annual grazing intensity dataset with 100 m resolution spanning from 1990–2020. These maps
144 can not only provide fundamental dataset with finer spatio-temporal resolution to address the limitations
145 of existing grazing intensity maps, but enhance a better understanding of sustainable management
146 practices as well as other grassland-related issues across the QTP.

147 **2 Data and methods**

148 **2.1 Study area**

149 Known as the Asia's water tower and the world's third pole, the QTP is geographically situated
150 between 73°19'–104°47' east longitude and 26°00'–39°47' north latitude, with a total area of about 2.61
151 million square kilometers (Figure 1). Its jurisdiction encompasses 182 counties within six provincial

152 regions of China, including Tibet Autonomous Region, Qinghai Province, Xinjiang Uygur Autonomous
153 Region, Gansu Province, Sichuan Province, and Yunnan Province (Meng et al., 2023). Elevation on the
154 QTP predominantly ranges between 3,000 m and 5,000 m, with an average altitude exceeding 4,000 m.
155 With grasslands constituting over half of its land cover, the QTP emerges as one of the most important
156 pastoral areas in China. Alpine steppe, alpine meadow, and temperate steppe characterize the main
157 grassland types on the QTP (Han et al., 2019; Zhai et al., 2022; Zhu et al., 2023b). The complex
158 geographical and climatic conditions of the QTP contributes to the markedly heterogeneous grassland
159 distribution, which correspondingly lead to the high heterogeneity in livestock distribution. Moreover,
160 social and economic development, coupled with policy initiatives directed towards grassland restoration,
161 have noticeably impacted the livestock numbers on the QTP over recent decades (Li et al., 2021; Li et al.,
162 2016).



163 Figure 1. The geographic zoning map of the Qinghai-Tibet Plateau (QTP) superposed with grassland vegetation.
164 Boundaries for the six provinces used for statistical analysis are also shown.

165 2.2 Data source

166 2.2.1 Census livestock data

167 The county-level census livestock data for the period between 1990 and 2020 were obtained from
168 the Bureau of Statistics of each county across the QTP (Table 1). The data includes the number of cattle,
169 sheep, horse and mule, with the exception of counties in Yunnan Province, which lack data for the
170 years from 1990 to 2007, and Ganzi Prefecture in Sichuan Province, which lack data for the years from
171 1990 to 1999, and Muli county in Sichuan Province, which lack data for the years from 1990 to 2007.
172 For these counties belonging to the same prefecture, including counties in Ganzi and Aba prefectures in
173 Sichuan Province, we used the livestock census data at the prefecture-level to carry out spatialization.
174 For these counties in Yunnan Province, since they belong to different municipalities, it is not reasonable
175 to replace them with municipal-level data. For these counties without livestock census data for some
176 years, we supplemented the missing data by linear interpolation with grazing density data in available
177 year. In total, livestock data were available for 182 counties, and 4,998 independent records were

178 finally generated. Furthermore, the respective quantities of different livestock types are converted to
 179 Standard Sheep Units (SU), in compliance with the Chinese national regulations (Meng et al., 2023).

180 Due to the difficulty of collecting township-level census livestock data, the validation data at the
 181 township scale collected in this study only involved these townships of Baching County (2010-2018)
 182 and Gaize County (2018-2020) in Tibet, and Hongyuan County in Sichuan Province (2008). The
 183 township-level census livestock data cumulatively involves 18 townships with a total of 112 records,
 184 and were only used for auxiliary validation of the simulation results.

185 The validation data at the pixel scale also encompass a total of 112 records from 68 sites, which
 186 were collected from literatures, questionnaires and field surveys. Specifically, 93 records at 49 sites
 187 spanning the 1990-2021 period were obtained from 17 literatures, 19 records at 19 sites were obtained
 188 from the questionnaires and the field survey in 2021. The detailed information for these records can be
 189 found in the Supplementary files (Figure S3 and Table S3).

190 Table 1. Summary of the livestock data used in this study

Variables	Scale	Time	Sources
Livestock numbers	County	1990-2020	Statistical bureau
	Township	2008-2020	Statistical bureau
	Pixel	1990-2021	Literatures, questionnaires and field surveys

191 *2.2.2 Factors affecting grazing activities*

192 Livestock grazing activities are often affected by abiotic and biotic resources, including climatic
 193 and environmental factors (Waha et al., 2018), herd foraging and grazing behaviours (Garrett et al.,
 194 2018; Miao et al., 2020). For instance, high-altitude and steep hillsides are unsuitable for grazing due to
 195 terrain constraints, and the distribution of herders directly affects the grazing areas (Luo et al., 2013;
 196 Mack et al., 2013; Robinson et al., 2014; Chen et al., 2019). Moreover, the livestock generally prefer
 197 areas abundant in water and pasture resources for foraging (Li et al., 2021). Therefore, in this study,
 198 topography, climatic, environmental and socio-economic impacts were considered as influential factors
 199 on grazing activities (Li et al., 2021; Meng et al., 2023).

200 We utilized correlation analysis and the Random Forest importance ranking tool to eliminate
 201 redundant environmental factors and determine the contribution of each factor. Ultimately, altitude,
 202 slope, distance to water source, population density, air temperature, precipitation and human-induced
 203 impacts on NPP (HNPP) was selected as indicators (Table 2). Specifically, elevation is derived from the
 204 DEM dataset accessible via the Resource and Environmental Data Cloud Platform of the Chinese
 205 Academy of Sciences (<https://www.gscloud.cn>), which also facilitated slope calculation. Rivers and
 206 lakes were obtained from the National Tibetan Plateau Data Center (<https://data.tpdc.ac.cn>), and the
 207 nearest Euclidean distance from each pixel to rivers or lakes is calculated accordingly. Meteorological
 208 elements such as daily air temperature and precipitation were downloaded from the China
 209 Meteorological Data Service Center (<http://data.cma.cn>). For the grid dataset that is not conditionally
 210 available, including population density, temperature, precipitation and HNPP, we detailed the creation
 211 process in the Supplementary file. All datasets utilized in this study were harmonized to consistent
 212 coordinate systems and resolutions (WGS 1984 Albers, 100 m).

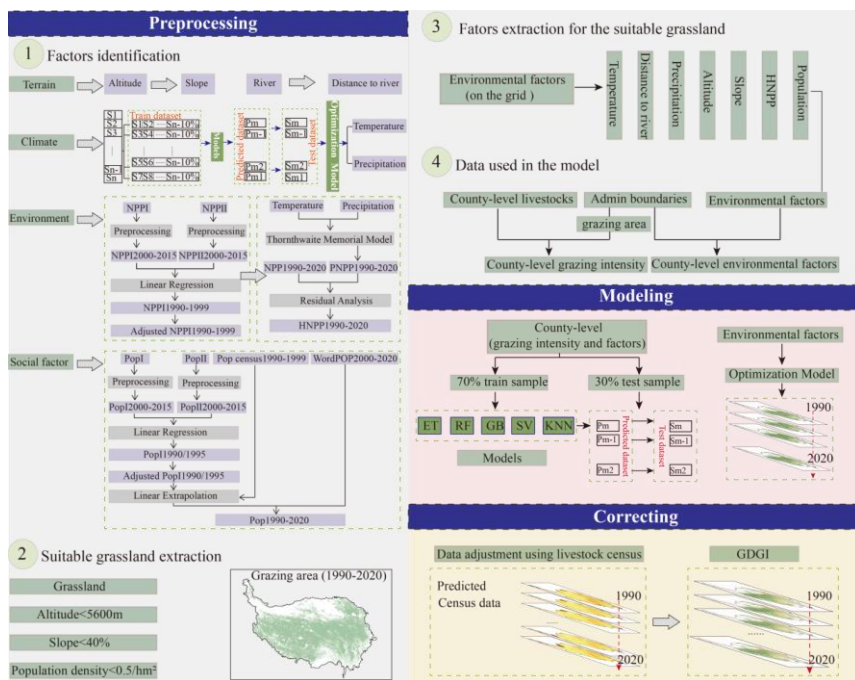
213 Table 2. Summary of factors affecting grazing activities on the QTP.

Variables	Format	Period	Time Resolution	Spatial Resolution	Source
-----------	--------	--------	--------------------	-----------------------	--------

Altitude	GeoTIFF	—	—	30m	https://www.gscloud.cn
Slope	GeoTIFF	—	—	30m	https://data.tpd.ac.cn
Water source	Shapefile	1990-2020	Annual	—	https://data.tpd.ac.cn
Population	GeoTIFF	1990-2020	Annual	100m	See supplementary file density
Temperature	GeoTIFF	1990-2020	Annual	100m	See supplementary file
Precipitation	GeoTIFF	1990-2020	Annual	100m	See supplementary file
HNPP	GeoTIFF	1990-2020	Annual	100m	See supplementary file

214 **2.3 Methodological framework**

215 We adopted a comprehensive methodological framework for mapping high-resolution grazing
 216 intensity on the QTP. [This study applied FAO’s assumption that the relationship between environmental](#)
 217 [factors and livestock intensity is identical at both the administrative and pixel level.](#) Three major steps
 218 are included to predict the distribution pattern of grazing intensity: (1) identifying factors affecting
 219 grazing activities and extracting theoretical suitable areas for livestock grazing, (2) building grazing
 220 spatialization model, and (3) filtering the model and correcting the grazing map. An exhaustive
 221 explanation of each step is provided in Figure 2.



222 Figure 2. Flowchart of creating grazing intensity maps using different methods and source products.
 223

224 2.3.1 Identifying factors and theoretical suitable areas for grazing

225 In this study, we assumed that grazing activities are confined solely to grassland. Consequently, the
226 potential grazing areas for each year were identified on the basis of grassland boundaries, which was
227 extracted from the 30 m annual land cover dataset (CLCD) (Yang and Huang, 2021). Furthermore,
228 grassland with slope over 40% and elevation higher than 5,600 m respectively, were considered
229 unsuitable for grazing and were therefore excluded from the potential grazing area in the subsequent
230 simulations (Robinson et al., 2014). In addition, the grassland with population density greater than 50
231 inhabitants km⁻² were also excluded (Li et al., 2018). The remaining isolated grassland was thus
232 categorized as theoretical feasible grazing regions.

233 The spatial patterns of abiotic and biotic resources, incorporating food availability, environmental
234 stress, and herder preference critically affect grazing activities (Meng et al., 2023). In light of this,
235 seven influencing factors in four aspects were selected for grazing intensity mapping (Figure 2-1).

236 2.3.2 Building grazing spatialization model

237 By performing regional statistics, the annual average values for each grazing influence factor were
238 extracted from the theoretically suitable grazing areas at the county scale, and were further used as
239 independent variables in the model construction. The dependent variable for the model was acquired by
240 determining the livestock density within each county, followed by a logarithmic transformation of the
241 values to normalize the distribution of the dependent variable. Consequently, a total of 4,998 samples
242 were derived from the aforementioned independent and dependent variables. Of these samples, 70%
243 were allocated for model training, while the remaining 30% comprised the test sets, serving to validate
244 the model's performance. Subsequently, we built grazing spatialization models using five machine
245 learning algorithms at the county scale, including Support Vector regression (SV) (Cortes and Vapnik,
246 1995; Lin et al., 2022), K-Nearest Neighbors (KNN) (Cover and Hart, 1967), Gradient Boosting
247 regression (GB) (Friedman, 2001; Pan et al., 2019), Random Forests (RF) (Breiman, 2001) and Extra
248 Trees regression (ET) (Geurts et al., 2006; Ahmad et al., 2018) (see Supplementary file for details).
249 Lastly, to assess the accuracy of the spatialized livestock map, the predicted livestock intensity values
250 were juxtaposed with the livestock statistical data from each respective county.

251 2.3.3 Correcting the grazing map

252 We further used the optimal model to predict the geographical distribution of grazing density across
253 the QTP. To maintain better consistency between the predicted livestock number and the census data,
254 the estimated results were adjusted using the census livestock numbers at the county scale as a control
255 according to Equation (1). Consequently, the corrected and refined map is presented as the final grazing
256 intensity map in this study.

257
$$L_{correction} = \frac{L_{CCensus}}{L_{Cgrid}} \times L_{grid} \quad (1)$$

258 where $L_{correction}$ is the predicted pixel-scale livestock number after adjustment, L_{Cgrid} represents the
259 estimated livestock number for each county, $L_{CCensus}$ is the census livestock number for each county,
260 and L_{grid} refers to the predicted livestock number at the pixel scale.

261 2.4 Accuracy evaluation

262 We used three accuracy validation indexes to evaluate the performance of five machine learning
263 algorithms, including coefficients of determination (R^2), mean absolute error (MAE), and root mean
264 square error (RMSE), by through a comparison of the predicted value with the census data. The
265 definitions of three metrics are presented in Equation (2) to (4).

$$266 R^2 = 1 - \frac{\sum_{i=1}^n (C_i - P_i)^2}{\sum_{i=1}^n (C_i - \bar{C})^2} \quad (2)$$

$$267 MAE = \frac{1}{n} \sum_{i=1}^n |C_i - P_i| \quad (3)$$

$$268 RMSE = \sqrt{\frac{1}{n} \sum_{i=1}^n (C_i - P_i)^2} \quad (4)$$

269 where C_i and P_i are the census livestock data and the predicted value for county i , respectively; \bar{C}
270 represents the mean census value for all county; and n gives the total number of counties.

271 2.5 uncertainties evaluation

272 Uncertainty in our grazing intensity maps can stem from multiple sources, such as the constraints of
273 cross-scale modeling and the intrinsic inaccuracies of the input data. To quantify these uncertainties, we
274 utilized the Monte Carlo (MC) method, conducting 100 iterations of simulation. Subsequently, we
275 evaluated uncertainty through the Mean Relative Error (MRE) and assessed the model's robustness
276 using the Standard Deviation (STD), following established methodologies (Yang et al., 2020;
277 Alexander et al., 2017; Mcmillan et al., 2018). The definitions for these metrics are delineated in
278 Equations (5) to (7).

$$279 MC = \frac{1}{n} \sum_{i=1}^n f(x_i) \quad (5)$$

$$280 MRE = \frac{1}{n} \sum_{i=1}^n \left| \frac{x_i - \bar{x}}{\bar{x}} \right| \quad (6)$$

$$281 STD = \frac{1}{n} \sum_{i=1}^n f(x_i) \sqrt{\frac{1}{n} \sum_{i=1}^n (x_i - \bar{x})^2} \quad (7)$$

282 where x_i are random samples, $f(x_i)$ is the function evaluated at x_i , and n is the number of
283 simulations. \bar{x} represents the mean value for all simulation maps.

284 3 Results

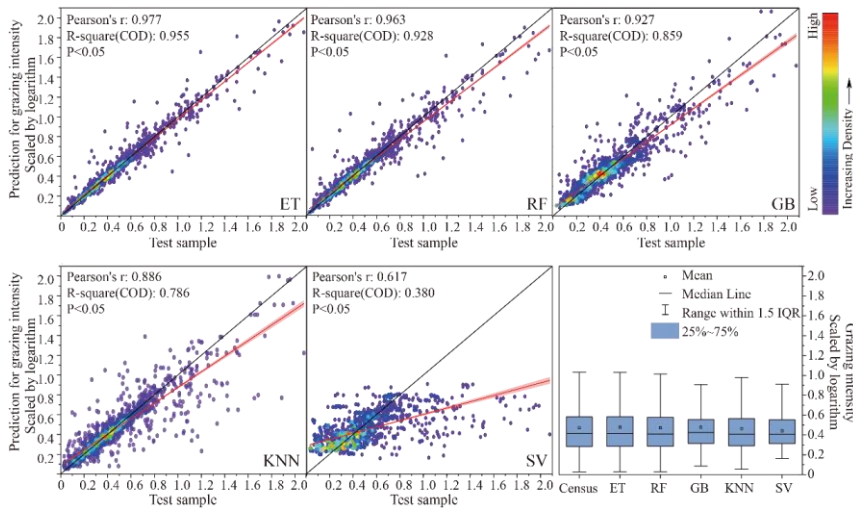
285 3.1 Performances of models

286 Table 3 summarizes the efficiency of the five used machine learning models with considering all
287 three accuracy evaluators of R^2 , MAE and RMSE. It can be seen that the ET model performs the best,
288 with its R^2 exceeding 0.955, and MAE (0.081 SU/hm²) and RMSE (0.164 SU/hm²) significantly lower
289 than the value of RF, GB, KNN and SVM models. Figure 3 illustrates the correlation between the
290 census livestock data and the livestock numbers predicted by the model for each county from 1990 to
291 2020. It demonstrated that the ET-predicted data displayed a distribution pattern consistent with that of
292 other models, but the scatter points of the ET model were more convergent to the 1:1 diagonal line,
293 indicating a superior fit compared to the other models. These comparisons suggest that the ET model
294 possesses superior robustness and can, therefore, provide stable estimations of livestock intensity on
295 the QTP.

296 Table 3. Comparison of mapping accuracy for five machine learning models based on the same validation datasets

Models	R^2	MAE (SU/hm ²)	RMSE (SU/hm ²)
ET	0.955	0.081	0.164
RF	0.928	0.099	0.208
GB	0.859	0.197	0.300
KNN	0.786	0.186	0.384
SVM	0.380	0.419	0.750

297 Note: The MAE and RMSE have calculated using inverse logarithmic transformation, presenting the
 298 actual values.



299 Figure 3. Scatterplots of model-predicted livestock numbers and census grazing data (scaled by logarithm) at the
 300 county sealelevel. The red solid line and the black solid line are the fitting line and the 1:1 diagonal line,
 301 respectively.
 302

格式化表格

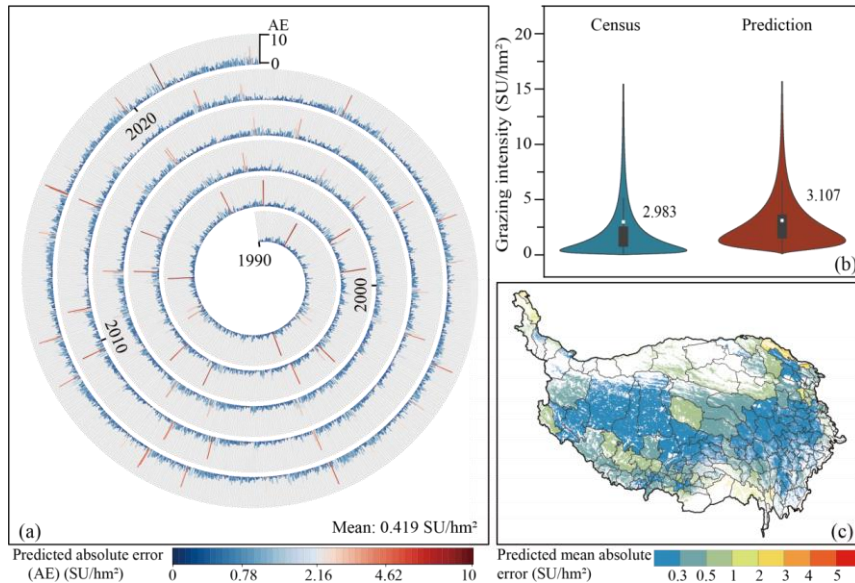
设置了格式: 字体: (默认) Times New Roman, (中文)
+中文正文 (宋体), 10 磅, 倾斜

设置了格式: 字体: (默认) Times New Roman, (中文)
+中文正文 (宋体), 10 磅

带格式的: 普通(网站), 段落间距段前: 0 磅, 行距:
单倍行距

设置了格式: 字体: 10 磅, 检查拼写和语法

设置了格式: 图案: 清除



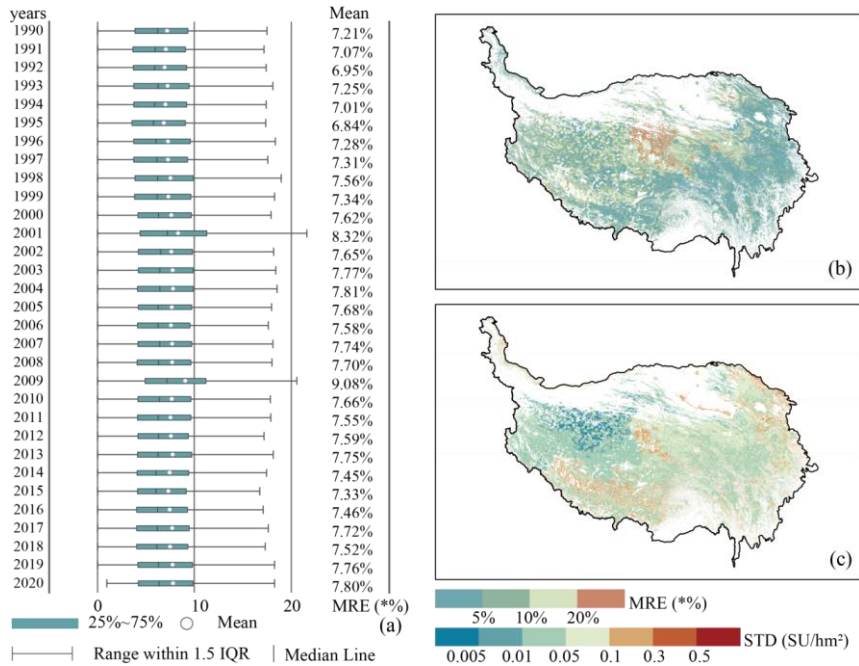
303
 304 Figure 4. Accuracy of the ET-predicted grazing intensity results at spatial resolution of 100 m from 1990 to 2020.
 305 (a) absolute error (AE) between the predicted and the census data at the county scale from 1990 to 2020; (b)
 306 comparison of the predicted and census data of the whole QTP from 1990 to 2020; (c) spatial distribution of the
 307 mean absolute error (MAE) during 1990 to 2020 for each county.

308 Using the ET model, we projected the spatio-temporal distribution of grazing intensity across the
 309 QTP from 1990 to 2020 at a $100\text{ m} \times 100\text{ m}$ resolution. To validate the accuracy of these predictive
 310 maps, we up scaled the pixel-level predictions to the county level and compared them against livestock
 311 census data (Figures 4a and 4b). The results clearly show a high degree of consistency between the
 312 predicted livestock intensity and the county-level census data, especially in areas with lower grazing
 313 intensity (Figures 4a and 4b). Specifically, while the mean census data indicated 2.983 SU/hm^2 for
 314 livestock intensity, our county-level predictions yielded an average of 3.106 SU/hm^2 , with a MAE of
 315 0.123 SU/hm^2 , a RMSE of 0.580 SU/hm^2 , and an R^2 value of 0.669 . Additionally, 76.31% of the
 316 counties ($n=3,814$) exhibited data discrepancies of no more than 0.6 SU/hm^2 , and 91.74% ($n=4,585$)
 317 had discrepancies under 1.0 SU/hm^2 . Regarding spatial distribution, areas with data discrepancies of
 318 less than 0.3 SU/hm^2 were predominantly located in the northwest and southeast regions of the QTP. In
 319 certain counties of the northeast and southwest, the variations were even below 1.0 SU/hm^2 (Figure 4c).

320 3.2 Evaluation of uncertainties

321 We have chosen the Mean Relative Error (MRE) as a key metric for evaluating the simulation
 322 accuracy of grazing intensity within the QTP. Employing Monte Carlo simulations spanning the period
 323 from 1990 to 2020, our research findings demonstrate that the average MRE for grazing intensity
 324 across the QTP ranged between 6.84% and 9.08% (Figure 5a). The spatial distribution of MRE
 325 indicates that the majority of the plateau exhibits low error margins. For example, in 2020, areas with
 326 an MRE of less than 5% accounted for 35.86% of the total grassland area, while those with an MRE
 327 below 10% constituted 75.84% . Only 3.38% of the grasslands had an MRE exceeding 20% , with these
 328 regions primarily located in the southwestern portion of the QTP (Figure 5b). Moreover, the robustness

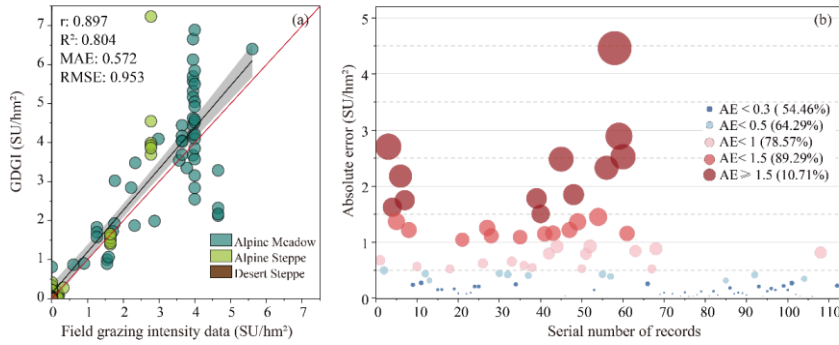
329 analysis suggests that the majority of regions within the QTP display relatively stable grazing intensity
 330 trends. For instance, the overall standard deviation (STD) in 2020 was 0.059 SU/hm², with the
 331 northwest region demonstrating remarkable stability, reflected in an STD of less than 0.005 SU/hm².
 332 Although some areas within the Yarlung Zangbo River Basin and the eastern part of Qinghai Province
 333 experienced higher variability, their STD was still maintained below 0.3 SU/hm² (Figure 5c).



334 |—| Range within 1.5 IQR | Median Line
 335 Figure 5. Uncertainty analysis of grazing intensity maps based on ET and Monte Carlo methods. (a) MRE of
 336 grazing intensity maps from 1990 to 2020, (b) spatial distribution of MRE, (c) spatial distribution of STD.

337 3.3 Validation of the GDGI dataset

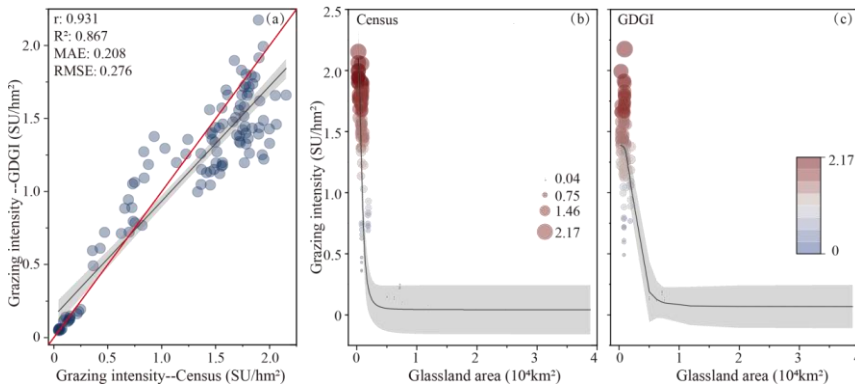
338 After employing county-level livestock census as a benchmark for quality control, we obtained the
 339 annual Gridded Dataset of Grazing Intensity maps (GDGI) across the QTP spanning 31 years from
 340 1990 to 2020. We firstly confirmed the accuracy of the GDGI dataset based on 112 field grazing
 341 intensity records at 68 sites (see Table S3 in Supplementary file for details), which ranged from 0 to
 342 5.61 sheep unit per hectare (SU/hm²), and covered three main grasslands on the QTP: the alpine steppe
 343 (N=62), alpine meadow (N=46), and alpine desert steppe (N=4). The GDGI dataset was assessed by
 344 undertaking a comparative accuracy assessment between it and the field grazing intensity data (Figure
 345 6a). It can be seen that in general, our dataset was highly consistent with the reference ground-truth
 346 validation data, with $R^2 = 0.804$, MAE = 0.572 SU/hm², and RMSE = 0.953 SU/hm². Moreover, the
 347 absolute errors between the GDGI data and the field grazing intensity data were relatively small, with
 348 more than half of the records having an error below 0.3 SU/hm², 78.57% below 1.0 SU/hm² and 89.29%
 349 below 1.5 SU/hm² (Figure 6b).



350

351 Figure 6. Validation of the GDGI dataset using 112 field grazing intensity records at the pixel scale: (a) linear
352 fitting results; (b) absolute error (AE) distribution.

353 We further validated the precision of the GDGI dataset using the township-level livestock census
354 data. Encouragingly, the evaluation results showed that the GDGI dataset has excellent performance at
355 the township scale (Figure 7a), with R^2 of 0.867, MAE of 0.208 SU/hm^2 , and RMSE of 0.276 SU/hm^2 .
356 In addition, similarly to the census data, the GDGI dataset indicated that some townships with few
357 grasslands area are still under high grazing pressure (Figure 7b and 7c).



358

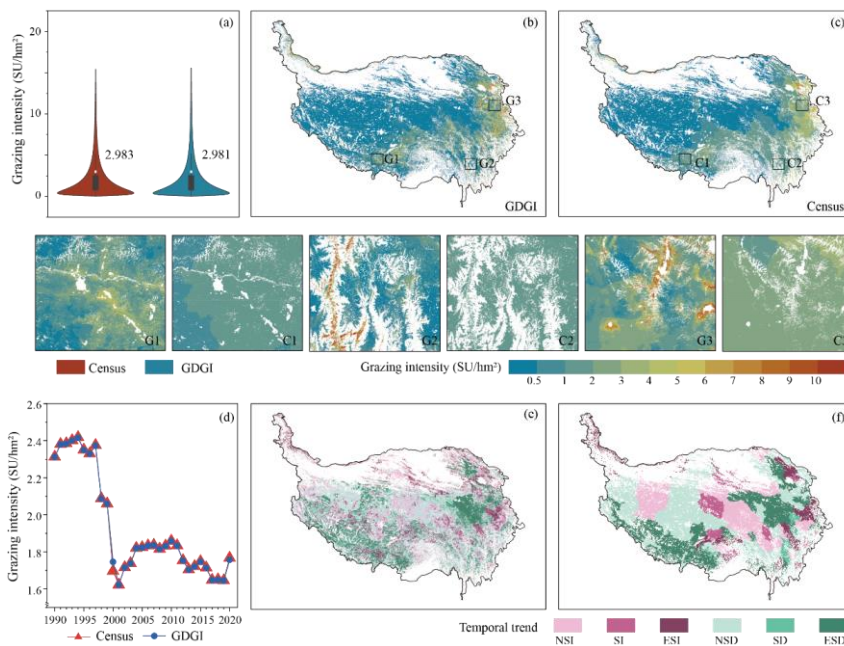
359 Figure 7. Validation of the GDGI dataset using census livestock data at the township level: (a) linear fit of
360 predicted number and census data; (b-c) logistic fit of grazing intensity data and grassland area.

361 3.4 Spatio-temporal variations of grazing intensity

362 In terms of the temporal trends of grazing intensity, the GDGI dataset overall exhibited consistent
363 trends with the livestock census data (Figure 8d-8f). Specifically, the census data indicated the
364 livestock numbers remained high and largely stable from 1990 to 1997, followed by a sharp decline
365 from 1997 to 2001, and then remained a period of fluctuation post-2001, which was successfully
366 captured by the GDGI dataset. Moreover, the spatial heterogeneity of grazing intensity within the
367 counties over the QTP was also effectively reflected by the GDGI dataset, a characteristic not
368 illustrated by the census dataset. For example, areas of high grazing intensity were concentrated in the

369 northeastern and south-central regions of the plateau, mainly including the eastern part of Qinghai
 370 Province, the southwestern part of Gansu Province, the northwestern part of Sichuan Province, and the
 371 eastern region of the Tibet Autonomous Region (Figure 8e and 8f).

372 Over the past 31 years, 63.95% of the plateau's grassland showed a decreasing trend in grazing
 373 intensity, with 49.80% showing significant decreases, primarily located in the eastern Sanjiangyuan
 374 area and the southwestern region of the QTP (Figure 8e and 8f). Meanwhile, grazing intensity was
 375 increasing in 36.05% of the grassland, but most of them (60.16%) did not reach the level of
 376 significance and were mainly distributed in the northeastern plateau (Figure 8e and 8f).



377
 378 Figure 8. Validation of the GDGI maps using the census grazing data from 1990 to 2020: (a) violin plot of the
 379 census data and the predicted value; (b-c) spatial distribution in SU per pixel; (d) temporal change in SU per year
 380 (only including 124 counties with livestock census data); (e-f) spatial distribution of SU changes tested by sen's
 381 slope and Mann-Kendall. Note: ESI for Extremely Significant Increase (slope>0 & $p<0.01$); SI for Significant
 382 Increase (slope_{>0} & $p<0.05$); NSI for Non-significant increase (slope>0 & $p>0.05$); ESD for Extremely
 383 Significant Decrease (slope<0 & $p<0.01$); SD for Significant decrease (slope<0 & $p<0.05$); NSD for
 384 Non-significant decrease (slope<0 & $p>0.05$).

385 4 Discussion

386 4.1 Comparison with other grazing intensity maps

387 To further assess the effectiveness and reliability of the developed GDGI dataset, the mapping
 388 results were juxtaposed with seven publicly available grazing intensity maps covering the QTP (Table
 389 4). It can be seen that despite their public availability, these maps lacked both in spatial and temporal

设置了格式: 字体: 倾斜
 设置了格式: 字体: 倾斜
 设置了格式: 字体: 倾斜
 设置了格式: 字体: 倾斜
 设置了格式: 字体: 倾斜
 设置了格式: 字体: 倾斜

390 resolution when juxtaposed with the GDGI maps. Our analysis was extended to four openly accessible
391 gridded livestock datasets, including GI-Sun (Sun et al., 2021), ALCC (Liu, 2021), GI-Meng (Meng
392 et al., 2023) and GLWs (Gilbert et al., 2018). A commonality among all five maps was the consistency
393 for the spatial patterns of grazing intensity, with prevalent high and low intensities in the northeast and
394 northwest regions, respectively (Figure 9). However, these maps differed significantly in terms of
395 accuracy. As the grazing intensity maps of GLWs and ALCC were produced based on the livestock
396 census data in 2001 and 2015, an accuracy comparison for the corresponding years was conducted
397 among the five datasets both at county and township scale. Observations at the county scale indicate
398 that all four datasets, with the exception of GI-Sun, are largely in alignment with the county census
399 data (Figure 9b). When examined at the township scale, GI-Sun and GLW demonstrate the most
400 significant discrepancies, with MRE surpassing 68%. ALCC and GI-Meng follow, recording MREs of
401 30.69% and 38.80%, respectively. Additionally, the GDGI shows the highest degree of accuracy in
402 relation to the township census data, as indicated by the lowest MAE and RMSE values (Figure 9c).
403 Moreover, the GDGI dataset spanning 31 years (1990–2020) earmarked it as a more suitable choice for
404 long-term studies in comparison to the other four datasets. Regarding spatial distribution, the overall
405 patterns of these grazing maps are largely consistent, exhibiting higher density patterns in the southeast
406 and lower in the northwest. However, notable discrepancies are still apparent in the finer details. In
407 general, in terms of visually representing the spatial distribution of livestock, the GDGI maps
408 exhibit the best performance.

409 ~~The above advantageous of the GDGI dataset are understandable. Several potential factors may~~
410 ~~contribute to the improved accuracy of the GDGI.~~ First, the livestock census data used in GDGI is
411 more detailed, aiding in enhancing the accuracy of the estimation results. Specifically, GI-sun, ALCC,
412 GI-Meng and GDGI all use county-level livestock statistics to map grazing intensity, whereas GLW3
413 and GLW4 are based on provincial-level census data to map, which results in their accuracy lagging
414 significantly behind the four other datasets (Nicolas et al., 2016; Sun et al., 2021). Second, grazing
415 densities are estimated by dividing the number of livestock from the statistical data, after a mask
416 excluding theoretical unsuitable grazing areas. However, these maps differ in their definitions of
417 suitable grazing areas. In this study, as with the GI-sun and GI-Meng maps, we considered grazing to
418 occur only on grasslands, and further excluded unsuitable areas such as high elevations and steep
419 slopes. This kind of definition is clearly more reasonable than the GLW series, which removed only
420 water bodies, urban core areas, and protected areas with relatively tight regulations of human activity
421 (Mcsherry and Ritchie, 2013; He et al., 2022). However, the GI-Meng dataset considers the core areas
422 of protected areas as grazing-free region, it does not match the actual situation on the QTP (Jiang et al.,
423 2023; Li et al., 2022b; Zhao et al., 2020). Those different thresholds for the definition of suitable
424 grazing areas are account for the fact each map has different theoretical grazing regions. ~~Third, the~~
425 ~~selection of models and environmental factors may also be a significant contributing factor, leading to~~
426 ~~variations in predictive accuracy. For instance, different algorithms were employed, including linear~~
427 ~~regression and machine learning methods (Nicolas et al., 2016; Li et al., 2021). Additionally, the~~
428 ~~environmental factors considered varied: specifically, the GDGI utilized the Human-induced Net~~
429 ~~Primary Productivity (HNPP) to represent grasslands, whereas other maps relied on Net Primary~~
430 ~~Productivity (NPP) and Normalized Difference Vegetation Index (NDVI) (Allred et al., 2013; Sun et al.,~~
431 ~~2021; Meng et al., 2023).~~ ~~Third, the selection of models and environmental factors may also be a~~
432 ~~contributing factor, which also leads to differences in prediction accuracy across maps. For instance,~~
433 ~~different algorithms were applied—linear regression and machine learning (Nicolas et al., 2016; Li et~~

域代码已更改

434 ~~al., 2021). The environmental factors also varied. Specifically, when representing grasslands, GDGI~~
435 ~~employed HNPP, whereas other maps used NPP and NDVI (Allred et al., 2013; Sun et al., 2021; Meng~~
436 ~~et al., 2023). Third, these maps decompose the livestock census data to pixels based on different~~
437 ~~mathematical theories, which also leads to differences in prediction accuracy across maps. Specifically,~~
438 ~~ALCC used a multivariate linear regression algorithm to predict grazing intensity, which has been~~
439 ~~shown to be significantly inferior to the RF machine learning method employed by GI-Meng, GLW3~~
440 ~~and GLW4 (Nicolas et al., 2016; Li et al., 2021). In this study, we used the ET model to predict~~
441 ~~livestock numbers and achieved higher accuracy accordingly. Finally, differences in the selection of~~
442 ~~factors affecting livestock distribution across maps may also lead to differences in map accuracy.~~
443 ~~Specifically, GI sun only used the NPP as indicator, but it is not simply linearly related to grazing~~
444 ~~intensity (Sun et al., 2021; Ma et al., 2022; Gilbert et al., 2018). ALCC considered the population~~
445 ~~density, NPP, and terrain as indicators, which are also incomplete considerations of the influencing~~
446 ~~factors. On the other hand, GLW series dataset considered 12 factors, such as NDVI, EVI, population~~
447 ~~distribution and elevation. GI-Meng dataset incorporated 14 factors including NDVI, soil PH, available~~
448 ~~nitrogen, available phosphorus, and available potassium. However, GLWs and GI-Meng ignored the~~
449 ~~decrease in the prediction accuracy due to redundancy among the factors. In this study, we selected~~
450 ~~factors related to grazing activities including terrain, climate, environment and social factor, and~~
451 ~~constructed a prediction model with seven factors including population density, elevation, climate, and~~
452 ~~HNPP. Unlike other livestock products, this study used HNPP for the first time to replace the~~
453 ~~commonly used NPP, or NDVI, or EVI as indicator, which has been proved to be more accurately~~
454 ~~expressed the relationship between livestock and grassland (Huang et al., 2022).~~

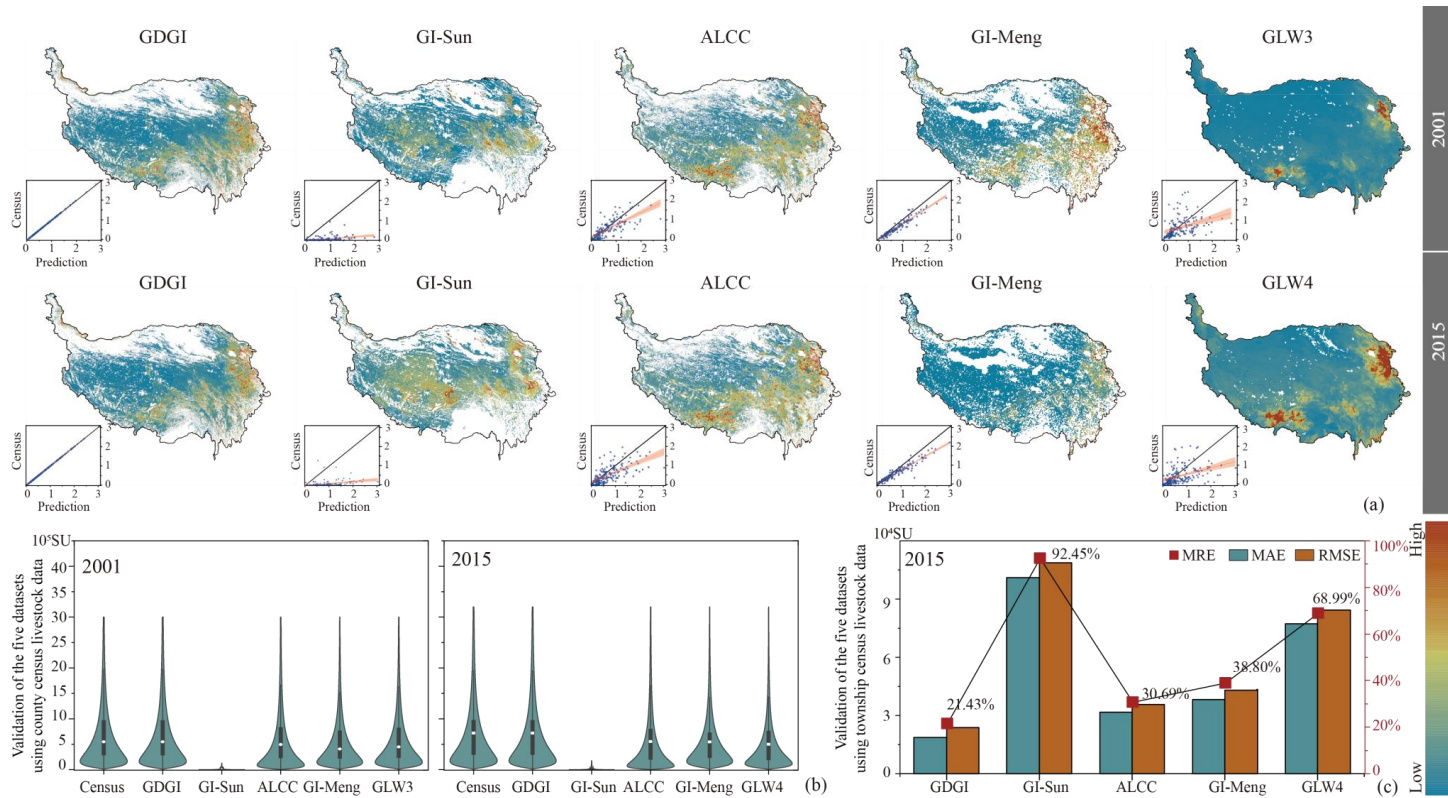
域代码已更改

设置了格式: 图案: 清除 (白色)

455 Table 4. Summary of map-derived parameters for this study and other seven public gridded livestock datasets covering the QTP.

Dataset	Accessibility	Census	Temporal resolution	Spatial resolution	Period (years)	Method	Livestock type
GDGI	Yes	County	annual	100 m	1990-2020 (31)	ET	Standard SU
GLW3	Yes	Province/sub-Province	annual	0.083°(≈10 km)	2001 (1)	RF	Cattle, ducks, pigs, chickens,
GLW4	Yes	Province/sub-Province	annual	0.083°(≈10 km)	2015 (1)	RF	sheep, goats
GI-Sun	Yes	County	five-year interval	1 km	1990-2015 (6)	LRA	Standard SU
ALCC	Yes	Province/sub-Province	annual	250 m	2000-2019 (20)	MLR	Standard SU
GI-Meng	Yes	County	annual	0.083°(≈10 km)	1982-2015 (34)	RF	Standard SU
GI-Li	No	County	five-year interval	1 km	2000-2015 (4)	DNN	Cattle and sheep
GI-Zhan	No	County	season	15'' (≈500 m)	2020 (2)	RF	Standard SU

456 Note: LRA is the abbreviation of linear regression analysis.



457

458 Figure 9. Comparisons of different grazing datasets for the years 2001 and 2015: (a) spatial patterns; (b) predicted livestock number and census data at county scale; (c) accuracy evaluation
 459 between predicted livestock number and census data at township scale.

460 4.2 Spatial heterogeneity of grazing intensities

461 In general, the multiyear average grazing intensity on the QTP increased from west to east during
462 1990 to 2020, with broad spatial heterogeneity (Figure 8). Highest grazing intensity was found mainly
463 in the northeastern and south-central regions of the Plateau (mostly higher than 5.0 SU/hm²), while
464 they were lowest in the northwest (mostly less than 1.0 SU/hm²). Over the past 31 years, the average
465 grazing intensity decreased across most of the Plateau, but 36.05% of the entire QTP grassland still
466 encountered continuous grazing intensity increase, especially in the northeastern regions (Figure 8).

467 The spatial heterogeneity of grazing intensities on the QTP may be attributed to the following
468 reasons. First, complex geographic and climatic conditions on the QTP determine the heterogeneity of
469 grassland, which in turn affects livestock distribution (Wang et al., 2018; Wei et al., 2022). In general,
470 the grazing intensity patterns shown in the GDGI maps are basically consistent with the stocking rate
471 threshold patterns in the QTP grasslands, both decreased from east to west (Zhu et al., 2023a). This
472 phenomenon partially reflects the heterogeneity of the grasslands, as the alpine meadows and the
473 steppes mainly distributed in the east and the west, respectively. Second, the dynamics of
474 socio-economic development are obviously another important factors determining grazing intensity. In
475 areas falling behind in terms of the socio-economic indicators, herders prefer to increase livestock in
476 efforts to improve household incomes, leading to greater pressure on grasslands in these regions (Fang
477 and Wu, 2022). In addition, the perceived increases in human population also resulted in the
478 considerably increased need to more livestock (Wei et al., 2022).

479 The grazing intensity dynamics across the QTP are partly reflective of the impacts of various
480 management policies that have been implemented over distinct periods. For example, a significant
481 increase in grazing intensity on the QTP was observed in the early 1990s, potentially a direct result of
482 the introduction of the household contract responsibility system. Moreover, the grazing intensity
483 experienced a pronounced decline from 1997 to 2001, as illustrated in Figure 8d, indicative of the
484 adverse effects of natural disasters. Notably, the severe snowstorms that struck Naqu in the central QTP
485 during 1997-1998 are documented to have caused the mortality of over 820,000 livestock (Ye et al.,
486 2020). Figure 8d further delineates a considerable upsurge in grazing intensity on the QTP between
487 2000 and 2010, aligning with the trends reported by Sun et al. (2021) and Li et al. (2021). This
488 observed increase may be attributed to a rebound in grazing activity following the aforementioned
489 natural disasters. In addition, Figure 8d indicates a sustained decrease in grazing intensity post-2010
490 across the plateau, which can be predominantly ascribed to the implementation of extensive ecological
491 conservation projects.

492 4.3 Implications for grazing management

493 Nearly half of the grasslands on the QTP have been reported to be degraded over the past four
494 decades (Wang et al., 2018; Dong et al., 2020), with some reports even indicating that the degraded
495 grassland has reached 90% (Wang et al., 2021). It is widely recognized that overgrazing is the
496 predominant and most pervasive unsustainable human activity continuing to drive grassland
497 degradation on the QTP (Wang et al., 2018; Chen et al., 2019). Generally, these degraded grassland on
498 the QTP can be effectively restored by adaptive management (Wang et al., 2022). However, better
499 management of grasslands requires a deeper understanding of the anthropogenic activities, which still
500 remain an important challenge and can be effectively addressed by the GDGI dataset.

501 According to the GDGI maps generated in this study, high-intensity grazing activities are mainly
502 concentrated in the northeastern as well as the south-central part of the QTP, with the grazing intensity
503 in some areas even nearly more than ten times than the average value of the entire plateau (Figure 6b),
504 and have exceeded the stocking rate threshold of these grasslands (Zhu et al., 2023a). Population
505 growth and the related increasing livelihood demands is one of the main reasons for this increase. To
506 meet daily needs and enhance household income, the herders have endeavored to increase livestock,
507 thereby intensifying grazing pressures on the grasslands over the QTP (Fang and Wu, 2022; Abu
508 Hammad and Tumeizi, 2012). Although the current average grazing intensity in the northwest QTP
509 (around 1.0 SU/hm²) is below their average stocking rate threshold (around 1.5 SU/hm²) (Zhu et al.,
510 2023a), the grassland management should still be given adequate attention. Because as the most arid
511 areas with low stocking rate threshold on the QTP, the grazing intensity in this region has been
512 increasing in recent years. Nevertheless, it must be noted that the stocking rate threshold may exceed
513 the carrying capacity, because it is predicted to lead to an extreme grassland degradation (Zhu et al.,
514 2023a). The GDGI dataset also showed a similar pattern between the grazing intensity data and the
515 WorldPop data near the built-up areas, indicating higher grazing intensity around settlements than other
516 regions on the QTP. In addition, the GDGI dataset also indicate that from 1990 to 2020, although the
517 grazing intensity of the Plateau has generally decreased, the hotspot areas for grazing activities have
518 remained almost unchanged. This implies that these regions should be the focus of adaptive grassland
519 management to effectively prevent grassland degradation, mainly based on the grass–livestock balance
520 which varies by time and space.

521 Encouragingly, the GDGI dataset show that the grazing intensity for two-thirds of the entire QTP
522 grassland decreased over the past 31 years, which is also consistent with other studies (Sun et al., 2021;
523 Li et al., 2021). Recent decades of biodiversity protection, active restoration projects as well as
524 management measures, such as nature reserves, grazing exclusion, part grazing ban combined with
525 fencing enclosure, are believed to have driven these decrease (Deng et al., 2017; Li and Bennett, 2019).
526 In addition, most grassland in the eastern Sanjiangyuan, the mid-eastern Changtang, and the northern
527 foothills of the Himalayas, showed a significant decrease with grazing intensity (Figure 6e), indicating
528 the importance of protected areas on preventing overstock and grassland degradation. Meanwhile, the
529 GDGI maps also show that the grazing density varies greatly among protected areas, possibly owing to
530 the difference in policy implementation. For instance, it can be seen from the GDGI maps that grazing
531 intensity are increasing in some protected areas, especially several wetland nature reserves on the Zoige
532 plateau (Figure 6e). Moreover, the average grazing intensity in all nature reserves on the QTP has
533 overall increased from 1990 to 2020, although their increase rate is much lower than the non-protected
534 areas (0.0125 SU/hm²·10a vs. 0.0304 SU/hm²·10a), which implies that grassland management in
535 protected areas still needs to be strengthened on the QTP.

536 The grazing initiatives in alignment with the Sustainable Development Goals (SDGs) on the QTP
537 can benefit from the GDGI dataset. Firstly, determination a reasonable stocking rate is vital to prevent
538 overstocking of the pastures, which will possibly induce extreme grassland degradation (Zhu et al.,
539 2023a). Stocking rate determination can be optimized by using our grazing intensity maps and the
540 stocking rate threshold maps of the QTP. Secondly, the GDGI maps can contribute to strategic
541 placement of fence, which is a common practice adopted to prevent grassland degradation on the QTP.
542 Building fences in areas with high grazing intensity and exceeding the carrying capacity can improve
543 the effectiveness of fence construction (Zhou et al., 2023; Zhang et al., 2023). Thirdly, the GDGI

设置了格式: 字体: 倾斜

544 dataset can provide a solid support for promoting effective nature reserve management, which in total
545 covering nearly one third of the entire QTP. For example, the GDGI maps showed that grazing
546 activities still exist in most nature reserves on the Plateau, although most of them have significantly
547 lower grazing intensities compared with their adjacent non-protected areas. By using the GDGI maps,
548 the conflict between ecological protection and grazing activities in nature reserves can be alleviated.
549 Finally, our grazing intensity maps can act as a basic dataset to support other grassland-related policies.
550 Currently, these policies on the QTP often adopt a one-size-fits-all approach to determine the carrying
551 capacity and carry out ecological compensation, which may lead to overstock or unfair financial
552 distribution (Wang et al., 2022). The grassland management strategies balancing carrying capacity and
553 stocking rates are more likely to result in optimal management choices for policymakers and
554 stakeholders, and our GDGI maps can contribute to this decision-making processes.

555 4.4 Uncertainties and limitations

556 Although this study has collected as reliable datasets as possible, users of the GDGI products
557 should be cognizant of inherent uncertainties and limitations within these datasets. Notably, the mean
558 relative error of the GDGI dataset spanning 1990 to 2020 was recorded at 4.2% (Figure 4a), calculated
559 from the average errors across 182 counties within the QTP that had accessible livestock census data.
560 Furthermore, approximately 8.26% of grassland areas exhibited a relative error exceeding 1.0 SU/hm²
561 (Figure 4b). Such discrepancies arise from several limitations that were subsequently propagated to the
562 final grazing intensity maps, thereby contributing to the dataset's overall uncertainties.

563 Firstly, the estimations of grazing intensities were fundamentally conservative, primarily due to the
564 lack of comprehensive input data. Livestock numbers, derived from year-end data at the county level,
565 inadvertently led to underestimations of grazing intensity by not accounting for livestock off-take rates.
566 Likewise, the evaluation focused solely on livestock grazing intensity, excluding wild herbivores and
567 forage-dependent livestock, which potentially underestimate actual grazing pressures on the QTP.
568 Additionally, despite identifying seven main factors influencing livestock distribution, the study did not
569 encompass all potential factors, such as fencing, forage availability, road proximity, and season
570 transformation in grazing practices. Moreover, to align with county-scale livestock census data, we
571 averaged the environmental factors at the county-scale. Although this approach have been widely used
572 on the hypothesis that a consistent causal relationship between livestock intensity and environmental
573 factors persists across various scales (Robinson et al., 2014; Nicolas et al., 2016; Li et al., 2021; Meng
574 et al., 2023), it might oversimplify the intricate dynamics between grazing intensity and lead to a
575 certain degree of estimation inaccuracies. In addition, the reliance on linear extrapolation to
576 Supplementary missing gridded 100-m population density data from 1990-1999 introduced further
577 uncertainties due to the limited resolution (1-km) and interval (5-year) of the ChinaPop dataset.

578 Secondly, the modeling process for mapping grazing intensity also suffered from several challenges.
579 Specifically, this study adopted the FAO's assumption that the relationship between environmental
580 factors and livestock intensity is uniform across both administrative and pixel levels. However, it is
581 unlikely that these relationships are entirely consistent across scales, and the county-level model's
582 approach inevitably smooths spatial details, potentially reducing the precision of the data. Furthermore,
583 for instance, this research employs the FAO's assumption that the relationship between environmental
584 factors and livestock intensity is identical at both the administrative and pixel level. Nevertheless, it is
585 improbable for the relationship at these two scales to be completely consistent, and the county level
586 model unavoidably smooths spatial details, leading to a reduction in data precision. What's more, the

设置了格式: 字体颜色: 自动设置

设置了格式: 字体颜色: 深红

ET model was trained with a limited sample size of 4,998 and applied to a vast area consisting of 150 million pixels, which could compromise the model's accuracy. In addition, despite the ET model's design to reduce overfitting risks by using randomly selected features and partition decision, the potential for overfit effects still remained, particularly when faced with a high number of output classes or insufficient sample sizes (Geurts et al., 2006; Galelli and Castelletti, 2013). In fact, this limitation was evident in this study, as the generalization capability of the ET model was restricted by the disparity between the number of training samples and the total number of pixels, leading to predictions that often exceeded actual livestock census (Figure 4a).

Thirdly, our methodological framework for high-resolution gridded grazing dataset mapping was developed based on the assumption that all grassland were accessible to livestock. However, in reality, the amount of available grassland was less due to fencing and grazing bans on the QTP (Zhan et al., 2023). Moreover, transhumant herders generally follow a seasonal calendar for summer pastures and winter pastures on the QTP. However, we did not consider this seasonal movements due to data limitations, which further restrict the analysis of seasonal livestock distribution patterns (Kolluru et al., 2023). Additionally, the model's reliance on human population as a proxy for livestock locations overlooked the possibility of high grazing intensity in areas with low human populations on the QTP, particularly in regions designated for summer pastures.

Finally, it is important to note that gathering livestock census data in the Qinghai-Tibet Plateau presents significant challenges, leading to a scarcity of livestock validation data in this study, particularly at the township and pixel scales. This limitation may, to some extent, impact the reliability of the grazing intensity data we have presented.

In summary, all these limitations associated with input data, the modeling process, and the methodological framework collectively contribute to the uncertainties and reduce accuracy of the GDGI maps. We henceforth recommend that future research should aim to incorporate more detailed data, consider additional influential factors, enhance key dataset's time-series consistency, and refine the methodological framework to improve the accuracy of grazing intensity mapping.

5 Data availability

The annual gridded grazing intensity maps of the QTP spanning from 1990 to 2020 are accessible at the following link: <https://doi.org/10.5281/zenodo.108511943141090> (Zhou et al., 2024). Each map is catalogued by year and recorded in GeoTIFF format, with values represented in SU/hm² per year. These datasets, with a spatial resolution of 100 m and annual temporal resolution, utilize the WGS-1984-Albers geographic coordinate system. To streamline data transfer and download processes, the comprehensive 31-year dataset has been compressed into a ZIP file, readily available for download and compatible with Geographic Information System (GIS) software for viewing.

6 Conclusions

In this study, we introduce a framework utilizing ET machine learning algorithms to achieve fine-scale livestock spatialization, subsequently generating the GDGI dataset across the QTP. The GDGI has a spatial resolution of 100 m and expands 31 years from 1990 to 2020. It is consistent with [county](#) livestock census data of the QTP, and ~~has a relatively higher precision than previous datasets~~

628 with MAE of 0.006 SU/hm² based on 4,998 independent test samples. In addition, the accuracy
629 evaluations at both pixel-level and township-level underscore the outstanding reliability and
630 applicability of the GDGI dataset, which can successfully capture the spatial heterogeneity and
631 variation in grazing intensities in greater details. Moreover, comparisons between the GDGI dataset and
632 other existing grazing map products further proved the robust and efficient of our dataset, and
633 demonstrate the validity of the proposed framework in the research of livestock spatialization.
634 Nonetheless, it is imperative for data users to recognize that the GDGI may still contain inherent
635 uncertainties. Our Monte Carlo simulations have estimated the average MRE for grazing intensity
636 across the QTP to vary between 6.84% and 9.08%. The GDGI dataset, as presented in this study, can
637 enhance the understanding of grazing activities on the QTP. This, in turn, can aid in the rational
638 utilization of grasslands and facilitate the implementation of informed and sustainable management
639 practices.
640 However, data users should be aware that the GDGI still harbors some potential uncertainties.
641 Monte Carlo simulations indicate that the average MRE for grazing intensity across the QTP ranged
642 from 6.84% to 9.08%. Notably, the data before 2001 show a sharp decline and should be interpreted
643 with caution. The GDGI dataset presented in this study can address existing limitations and enhance the
644 understanding of grazing activities on the QTP. This, in turn, can aid in the rational utilization of
645 grasslands and facilitate the implementation of informed and sustainable management practices.

设置了格式: 字体颜色: 自动设置

设置了格式: 字体: (默认) Times New Roman, 10 磅,
字体颜色: 红色

646 **Supplementary.**

647 For gridded datasets influencing grazing that are not directly available, or that do not meet
648 spatio-temporal resolution requirements—such as those pertaining to population density, temperature,
649 precipitation, and HNPP—we have delineated the processing or creation procedures in the
650 Supplementary file.

651 **Author contributions.**

652 T.L. conceived the research; J.Z. and J.N. performed the analyses and wrote the first draft of the
653 paper; N.W. and T.L. reviewed and edited the paper before submission. All authors made substantial
654 contributions to the discussion of content.

655 **Competing interests.**

656 The authors declare that they have no conflict of interest.

657 **Acknowledgements.**

658 We would like to thank the Bureau of Statistics of each county over the QTP for providing the
659 census livestock data.

660 **Financial support.**

661 This research was supported by the Second Tibetan Plateau Scientific Expedition and Research
662 Program (STEP), Ministry of Science and Technology of the People's Republic of China (grant no.

663 2019QZKK0402) and the National Natural Science Foundation of China (grant no. 42071238).

664 **References**

- 665 Abu Hammad, A. and Tumeizi, A.: Land degradation: socioeconomic and environmental causes and
666 consequences in the eastern Mediterranean, *Land. Degrad. Dev.*, 23, 216-226,
667 <https://doi.org/10.1002/ldr.1069>, 2012.
- 668 Ahmad, M. W., Reynolds, J., and Rezgui, Y.: Predictive modelling for solar thermal energy systems: A
669 comparison of support vector regression, random forest, extra trees and regression trees, *J. Clean.*
670 *Prod.*, 203, 810-821, <https://doi.org/10.1016/j.jclepro.2018.08.207>, 2018.
- 671 Alexander, P., Prestele, R., Verburg, P. H., Armeth, A., Baranzelli, C., Batista e Silva, F., Brown, C.,
672 Butler, A., Calvin, K., and Dendoncker, N.: Assessing uncertainties in land cover projections, *Glob.*
673 *Chang. Biol.*, 23, 767-781, 2017.
- 674 Allred, B. W., Fuhlendorf, S. D., Hovick, T. J., Dwayne Elmore, R., Engle, D. M., and Joern, A.:
675 Conservation implications of native and introduced ungulates in a changing climate, *Glob. Chang.*
676 *Biol.*, 19, 1875-1883, <https://doi.org/10.1111/gcb.12183>, 2013.
- 677 Breiman, L.: Random Forests, *Mach. Learn.*, 45, 5-32, <https://doi.org/10.1023/A:1010933404324>,
678 2001.
- 679 Cai, Y. J., Wang, X. D., Tian, L. L., Zhao, H., Lu, X. Y., and Yan, Y.: The impact of excretal returns
680 from yak and Tibetan sheep dung on nitrous oxide emissions in an alpine steppe on the
681 Qinghai-Tibetan Plateau, *Soil. Biol. Biochem.*, 76, 90-99,
682 <https://doi.org/10.1016/j.soilbio.2014.05.008>, 2014.
- 683 Chang, J. F., Ciais, P., Gasser, T., Smith, P., Herrero, M., Havlík, P., Obersteiner, M., Guenet, B., Goll,
684 D. S., Li, W., Naipal, V., Peng, S. S., Qiu, C. J., Tian, H. Q., Viovy, N., Yue, C., and Zhu, D.: Climate
685 warming from managed grasslands cancels the cooling effect of carbon sinks in sparsely grazed and
686 natural grasslands, *Nat. Commun.*, 12, 118, <https://doi.org/10.1038/s41467-020-20406-7>, 2021.
- 687 Chen, Y. Z., Ju, W. M., Mu, S. J., Fei, X. R., Cheng, Y., Propastin, P., Zhou, W., Liao, C. J., Chen, L. X.,
688 Tang, R. J., Qi, J. G., Li, J. L., and Ruan, H. H.: Explicit Representation of Grazing Activity in a
689 Diagnostic Terrestrial Model: A Data - Process Combined Scheme, *J. Adv. Model. Earth. Sy.*, 11,
690 957-978, <https://doi.org/10.1029/2018ms001352>, 2019.
- 691 Cortes, C. and Vapnik, V.: Support-vector networks, *Mach. Learn.*, 20, 273-297,
692 <https://doi.org/10.1007/BF00994018>, 1995.
- 693 Cover, T. and Hart, P.: Nearest neighbor pattern classification, *Ieee. T. Inform. Theory.*, 13, 21-27,
694 <https://doi.org/10.1109/TIT.1967.1053964>, 1967.
- 695 Dara, A., Baumann, M., Freitag, M., Hölzel, N., Hostert, P., Kamp, J., Müller, D., Prishchepov, A. V.,
696 and Kuemmerle, T.: Annual Landsat time series reveal post-Soviet changes in grazing pressure,
697 *Remote. Sens. Environ.*, 239, 111667, <https://doi.org/10.1016/j.rse.2020.111667>, 2020.
- 698 Deng, L., Zhou, S. G., Wu, P., Gao, L., and Chang, X.: Effects of grazing exclusion on carbon
699 sequestration in China's grassland, *Earth-Sci. Rev.*, 173, 84-95,
700 <https://doi.org/10.1016/j.earscirev.2017.08.008>, 2017.
- 701 Dong, S. K., Shang, Z. H., Gao, J. X., and Boone, R. B.: Enhancing sustainability of grassland
702 ecosystems through ecological restoration and grazing management in an era of climate change on
703 Qinghai-Tibetan Plateau, *Agr. Ecosyst. Environ.*, 287, 106684,
704 <https://doi.org/10.1016/j.agee.2019.106684>, 2020.

705 Fang, X. N. and Wu, J. G.: Causes of overgrazing in Inner Mongolian grasslands: Searching for deep
706 leverage points of intervention, *Ecol. Soc.*, 27, <https://doi.org/10.5751/es-12878-270108>, 2022.

707 Feng, R. Z., Long, R. J., Shang, Z. H., Ma, Y. S., Dong, S. K., and Wang, Y. L.: Establishment of
708 *Elymus natans* improves soil quality of a heavily degraded alpine meadow in Qinghai-Tibetan
709 Plateau, China, *Plant. Soil.*, 327, 403-411, <https://doi.org/10.1007/s11104-009-0065-3>, 2009.

710 Fetzel, T., Havlik, P., Herrero, M., Kaplan, J. O., Kastner, T., Kroisleitner, C., Rolinski, S., Searchinger,
711 T., Van Bodegom, P. M., Wirseniuss, S., and Erb, K. H.: Quantification of uncertainties in global
712 grazing systems assessment, *Global. Biogeochem. Cy.*, 31, 1089-1102,
713 <https://doi.org/10.1002/2016gb005601>, 2017.

714 Friedman, J. H.: Greedy function approximation: a gradient boosting machine, *Ann. Stat.*, 29,
715 1189-1232, <https://doi.org/10.1214/aos/1013203451>, 2001.

716 Galelli, S. and Castelletti, A.: Assessing the predictive capability of randomized tree-based ensembles
717 in streamflow modelling, *Hydrol. Earth. Syst. Sc.*, 17, 2669-2684,
718 <https://doi.org/10.5194/hess-17-2669-2013>, 2013.

719 García, R., Aguilar, J., Toro, M., Pinto, A., and Rodríguez, P.: A systematic literature review on the use
720 of machine learning in precision livestock farming, *Comput. Electron. Agr.*, 179, 105826,
721 <https://doi.org/10.1016/j.compag.2020.105826>, 2020.

722 García Ruiz, J. M., Tomás Faci, G., Diarte Blasco, P., Montes, L., Domingo, R., Sebastián, M., Lasanta,
723 T., González Sampérez, P., López Moreno, J. I., Arnáez, J., and Beguería, S.: Transhumance and
724 long-term deforestation in the subalpine belt of the central Spanish Pyrenees: An interdisciplinary
725 approach, *Catena.*, 195, 104744, <https://doi.org/10.1016/j.catena.2020.104744>, 2020.

726 Garrett, R. D., Koh, I., Lambin, E. F., le Polain de Waroux, Y., Kastens, J. H., and Brown, J. C.:
727 Intensification in agriculture-forest frontiers: Land use responses to development and conservation
728 policies in Brazil, *Global. Environ. Chang.*, 53, 233-243,
729 <https://doi.org/10.1016/j.gloenvcha.2018.09.011>, 2018.

730 Geurts, P., Ernst, D., and Wehenkel, L.: Extremely randomized trees, *Mach. Learn.*, 63, 3-42,
731 <https://doi.org/10.1007/s10994-006-6226-1>, 2006.

732 Gilbert, M., Nicolas, G., Cinardi, G., Van Boeckel, T. P., Vanwambeke, S. O., Wint, G. R. W., and
733 Robinson, T. P.: Global distribution data for cattle, buffaloes, horses, sheep, goats, pigs, chickens and
734 ducks in 2010, *Sci. Data.*, 5, 180227, <https://doi.org/10.1038/sdata.2018.227>, 2018.

735 Godfray, H. C. J., Aveyard, P., Garnett, T., Hall, J. W., Key, T. J., Lorimer, J., Pierrehumbert, R. T.,
736 Scarborough, P., Springmann, M., and Jebb, S. A.: Meat consumption, health, and the environment,
737 *Science.*, 361, 243, <https://doi.org/10.1126/science.aam5324>, 2018.

738 Guo, Z. L., Li, Z., and Cui, G. F.: Effectiveness of national nature reserve network in representing
739 natural vegetation in mainland China, *Biodivers. Conserv.*, 24, 2735-2750,
740 <https://doi.org/10.1007/s10531-015-0959-8>, 2015.

741 Han, Y. H., Dong, S. K., Zhao, Z. Z., Sha, W., Li, S., Shen, H., Xiao, J. N., Zhang, J., Wu, X. Y., Jiang,
742 X. M., Zhao, J. B., Liu, S. L., Dong, Q. M., Zhou, H. K., and Yeomans, J. C.: Response of soil
743 nutrients and stoichiometry to elevated nitrogen deposition in alpine grassland on the
744 Qinghai-Tibetan Plateau, *Geoderma.*, 343, 263-268, <https://doi.org/10.1016/j.geoderma.2018.12.050>,
745 2019.

746 He, M., Pan, Y. H., Zhou, G. Y., Barry, K. E., Fu, Y. L., and Zhou, X. H.: Grazing and global change
747 factors differentially affect biodiversity - ecosystem functioning relationships in grassland
748 ecosystems, *Glob. Chang. Biol.*, 28, 5492-5504, <https://doi.org/10.1111/gcb.16305>, 2022.

749 Heddam, S., Ptak, M., and Zhu, S. L.: Modelling of daily lake surface water temperature from air
750 temperature: Extremely randomized trees (ERT) versus Air2Water, MARS, M5Tree, RF and
751 MLPNN, *J. Hydrol.*, 588, 125130, <https://doi.org/10.1016/j.jhydrol.2020.125130>, 2020.

752 Hu, Y., Cheng, H., and Tao, S.: Environmental and human health challenges of industrial livestock and
753 poultry farming in China and their mitigation, *Environ. Int.*, 107, 111-130,
754 <https://doi.org/10.1016/j.envint.2017.07.003>, 2017.

755 Huang, X. T., Yang, Y. S., Chen, C. B., Zhao, H. F., Yao, B. Q., Ma, Z., Ma, L., and Zhou, H. K.:
756 Quantifying and Mapping Human Appropriation of Net Primary Productivity in Qinghai Grasslands
757 in China, *Agriculture.*, 12, 483, <https://doi.org/10.3390/agriculture12040483>, 2022.

758 Humpenöder, F., Bodirsky, B. L., Weindl, I., Lotze Campen, H., Linder, T., and Popp, A.: Projected
759 environmental benefits of replacing beef with microbial protein, *Nature.*, 605, 90-96,
760 <https://doi.org/10.1038/s41586-022-04629-w>, 2022.

761 Jiang, M. J., Zhao, X. F., Wang, R., Yin, L., and Zhang, B. L.: Assessment of Conservation
762 Effectiveness of the Qinghai–Tibet Plateau Nature Reserves from a Human Footprint Perspective
763 with Global Lessons, *Land.*, 12, 869, <https://doi.org/10.3390/land12040869>, 2023.

764 Kolluru, V., John, R., Saraf, S., Chen, J. Q., Hankerson, B., Robinson, S., Kussainova, M., and Jain, K.:
765 Gridded livestock density database and spatial trends for Kazakhstan, *Sci. Data.*, 10, 839,
766 <https://doi.org/10.1038/s41597-023-02736-5>, 2023.

767 Kumar, P., Abubakar, A. A., Verma, A. K., Umaraw, P., Adewale Ahmed, M., Mehta, N., Nizam Hayat,
768 M., Kaka, U., and Sazili, A. Q.: New insights in improving sustainability in meat production:
769 opportunities and challenges, *Crit. Rev. Food. Sci.*, 1-29,
770 <https://doi.org/10.1080/10408398.2022.2096562>, 2022.

771 Li, M. Q., Liu, S. L., Wang, F. F., Liu, H., Liu, Y. X., and Wang, Q. B.: Cost-benefit analysis of
772 ecological restoration based on land use scenario simulation and ecosystem service on the
773 Qinghai-Tibet Plateau, *Glob. Ecol. Conserv.*, 34, e02006,
774 <https://doi.org/10.1016/j.gecco.2022.e02006>, 2022a.

775 Li, P. and Bennett, J.: Understanding herders' stocking rate decisions in response to policy initiatives,
776 *Sci. Total. Environ.*, 672, 141-149, <https://doi.org/10.1016/j.scitotenv.2019.03.407>, 2019.

777 Li, Q., Zhang, C. L., Shen, Y. P., Jia, W. R., and Li, J.: Quantitative assessment of the relative roles of
778 climate change and human activities in desertification processes on the Qinghai-Tibet Plateau based
779 on net primary productivity, *Catena.*, 147, 789-796, <https://doi.org/10.1016/j.catena.2016.09.005>,
780 2016.

781 Li, S., Wu, J., Gong, J., and Li, S.: Human footprint in Tibet: Assessing the spatial layout and
782 effectiveness of nature reserves, *Sci Total Environ*, 621, 18-29,
783 <https://doi.org/10.1016/j.scitotenv.2017.11.216>, 2018.

784 Li, T., Cai, S. H., Singh, R. K., Cui, L. Z., Fava, F., Tang, L., Xu, Z. H., Li, C. J., Cui, X. Y., Du, J. Q.,
785 Hao, Y. B., Liu, Y. X., and Wang, Y. F.: Livelihood resilience in pastoral communities:
786 Methodological and field insights from Qinghai-Tibetan Plateau, *Sci. Total. Environ.*, 838, 155960,
787 <https://doi.org/10.1016/j.scitotenv.2022.155960>, 2022b.

788 Li, X. H., Hou, J. L., and Huang, C. L.: High-Resolution Gridded Livestock Projection for Western
789 China Based on Machine Learning, *Remote. Sens.*, 13, 5038, <https://doi.org/10.3390/rs13245038>,
790 2021.

791 Lin, G. C., Lin, A. J., and Gu, D. L.: Using support vector regression and K-nearest neighbors for
792 short-term traffic flow prediction based on maximal information coefficient, *Inform. Sciences.*, 608,

793 517-531, <https://doi.org/10.1016/j.ins.2022.06.090>, 2022.

794 [Liu, B. T.: Actual livestock carrying capacity estimation product in Qinghai-Tibet Plateau \(2000-2019\).](#)

795 [National Tibetan Plateau Data Center. \[Dataset\]. \[https://doi.org/10.11888/Ecolo.tpd.c.271513.\]\(https://doi.org/10.11888/Ecolo.tpd.c.271513.2021\)](#)

796 [2021.](#)

797 Long, S. J., Wei, X. L., Zhang, F., Zhang, R. H., Xu, J., Wu, K., Li, Q. Q., and Li, W. W.: Estimating

798 daily ground-level NO₂ concentrations over China based on TROPOMI observations and machine

799 learning approach, *Atmos. Environ.*, 289, 119310, <https://doi.org/10.1016/j.atmosenv.2022.119310>,

800 2022.

801 Luo, J. F., Hoogendoorn, C., van der Weerden, T., Saggarr, S., de Klein, C., Giltrap, D., Rollo, M., and

802 Rys, G.: Nitrous oxide emissions from grazed hill land in New Zealand, *Agr. Ecosyst. Environ.*, 181,

803 58-68, <https://doi.org/10.1016/j.agee.2013.09.020>, 2013.

804 Ma, C., Xie, Y., Duan, H., Wang, X., Bie, Q., Guo, Z., He, L., and Qin, W.: Spatial quantification

805 method of grassland utilization intensity on the Qinghai-Tibetan Plateau: A case study on the Selinco

806 basin, *J. Environ. Manage.*, 302, 114073, <https://doi.org/10.1016/j.jenvman.2021.114073>, 2022.

807 Mack, G., Walter, T., and Flury, C.: Seasonal alpine grazing trends in Switzerland: Economic

808 importance and impact on biotic communities, *Environ. Sci. Policy.*, 32, 48-57,

809 <https://doi.org/10.1016/j.envsci.2013.01.019>, 2013.

810 Martinuzzi, S., Radeloff, V. C., Pastur, G. M., Rosas, Y. M., Lizarraga, L., Politi, N., Rivera, L., Herrera,

811 A. H., Silveira, E. M. O., Olah, A., and Pidgeon, A. M.: Informing forest conservation planning with

812 detailed human footprint data for Argentina, *Glob. Ecol. Conserv.*, 31, e01787,

813 <https://doi.org/10.1016/j.gecco.2021.e01787>, 2021.

814 McMillan, H. K., Westerberg, I. K., and Krueger, T.: Hydrological data uncertainty and its implications,

815 *Wiley Interdisciplinary Reviews: Water*, 5, e1319, 2018.

816 McSherry, M. E. and Ritchie, M. E.: Effects of grazing on grassland soil carbon: a global review, *Glob.*

817 *Chang. Biol.*, 19, 1347-1357, <https://doi.org/10.1111/gcb.12144>, 2013.

818 Meng, N., Wang, L. J., Qi, W. C., Dai, X. H., Li, Z. Z., Yang, Y. Z., Li, R. N., Ma, J. F., and Zheng, H.:

819 A high-resolution gridded grazing dataset of grassland ecosystem on the Qinghai-Tibet Plateau in

820 1982-2015, *Sci. Data.*, 10, 68, <https://doi.org/10.1038/s41597-023-01970-1>, 2023.

821 Miao, L. J., Sun, Z. L., Ren, Y. J., Schierhorn, F., and Müller, D.: Grassland greening on the Mongolian

822 Plateau despite higher grazing intensity, *Land. Degrad. Dev.*, 32, 792-802,

823 <https://doi.org/10.1002/ldr.3767>, 2020.

824 Minoofar, A., Gholami, A., Eslami, S., Hajizadeh, A., Gholami, A., Zandi, M., Ameri, M., and Kazem,

825 H. A.: Renewable energy system opportunities: A sustainable solution toward cleaner production and

826 reducing carbon footprint of large-scale dairy farms, *Energ. Convers. Manage.*, 293, 117554,

827 <https://doi.org/10.1016/j.enconman.2023.117554>, 2023.

828 Mulligan, M., van Soesbergen, A., Hole, D. G., Brooks, T. M., Burke, S., and Hutton, J.: Mapping

829 nature's contribution to SDG 6 and implications for other SDGs at policy relevant scales, *Remote.*

830 *Sens. Environ.*, 239, 111671, <https://doi.org/10.1016/j.rse.2020.111671>, 2020.

831 Muloi, D. M., Wee, B. A., McClean, D. M. H., Ward, M. J., Pankhurst, L., Phan, H., Ivens, A. C.,

832 Kivali, V., Kiyong'a, A., Ndinda, C., Gitahi, N., Ouko, T., Hassell, J. M., Imboma, T., Akoko, J.,

833 Murungi, M. K., Njoroge, S. M., Muinde, P., Nakamura, Y., Alumasa, L., Furmaga, E., Kaitho, T.,

834 Öhgren, E. M., Amanya, F., Ogendo, A., Wilson, D. J., Bettridge, J. M., Kiiru, J., Kyobutungi, C.,

835 Tacoli, C., Kang'ethe, E. K., Davila, J. D., Kariuki, S., Robinson, T. P., Rushton, J., Woolhouse, M. E.

836 J., and Fèvre, E. M.: Population genomics of *Escherichia coli* in livestock-keeping households across

带格式的: 缩进: 左侧: 0 厘米, 悬挂缩进: 2 字符,
首行缩进: -2 字符

设置了格式: 超链接, 字体: (默认) Calibri, 检查拼
写和语法

837 a rapidly developing urban landscape, *Nat. Microbiol.*, 7, 581-589,
838 <https://doi.org/10.1038/s41564-022-01079-y>, 2022.

839 Neumann, K., Elbersen, B. S., Verburg, P. H., Staritsky, I., Pérez-Soba, M., de Vries, W., and Rienks, W.
840 A.: Modelling the spatial distribution of livestock in Europe, *Landscape. Ecol.*, 24, 1207-1222,
841 <https://doi.org/10.1007/s10980-009-9357-5>, 2009.

842 Nicolas, G., Robinson, T. P., Wint, G. R., Conchedda, G., Cinardi, G., and Gilbert, M.: Using Random
843 Forest to Improve the Downscaling of Global Livestock Census Data, *Plos. One.*, 11, e0150424,
844 <https://doi.org/10.1371/journal.pone.0150424>, 2016.

845 O'Neill, D. W. and Abson, D. J.: To settle or protect? A global analysis of net primary production in
846 parks and urban areas, *Ecol. Econ.*, 69, 319-327, <https://doi.org/10.1016/j.ecolecon.2009.08.028>,
847 2009.

848 Pan, Y. J., Chen, S. Y., Qiao, F. X., Ukkusuri, S. V., and Tang, K.: Estimation of real-driving emissions
849 for buses fueled with liquefied natural gas based on gradient boosted regression trees, *Sci. Total.*
850 *Environ.*, 660, 741-750, <https://doi.org/10.1016/j.scitotenv.2019.01.054>, 2019.

851 Petz, K., Alkemade, R., Bakkenes, M., Schulp, C. J. E., van der Velde, M., and Leemans, R.: Mapping
852 and modelling trade-offs and synergies between grazing intensity and ecosystem services in
853 rangelands using global-scale datasets and models, *Global. Environ. Chang.*, 29, 223-234,
854 <https://doi.org/10.1016/j.gloenvcha.2014.08.007>, 2014.

855 Pozo, R. A., Cusack, J. J., Acebes, P., Malo, J. E., Traba, J., Iranzo, E. C., Morris-Trainor, Z.,
856 Minderman, J., Bunnefeld, N., Radic-Schilling, S., Moraga, C. A., Arriagada, R., and Corti, P.:
857 Reconciling livestock production and wild herbivore conservation: challenges and opportunities,
858 *Trends. Ecol. Evol.*, 36, 750-761, <https://doi.org/10.1016/j.tree.2021.05.002>, 2021.

859 Prosser, D. J., Wu, J., Ellis, E. C., Gale, F., Van Boeckel, T. P., Wint, W., Robinson, T., Xiao, X., and
860 Gilbert, M.: Modelling the distribution of chickens, ducks, and geese in China, *Agric Ecosyst*
861 *Environ.*, 141, 381-389, <https://doi.org/10.1016/j.agee.2011.04.002>, 2011.

862 Robinson, T. P., Wint, G. R., Conchedda, G., Van Boeckel, T. P., Ercoli, V., Palamara, E., Cinardi, G.,
863 D'Aiotti, L., Hay, S. I., and Gilbert, M.: Mapping the global distribution of livestock, *Plos. One.*, 9,
864 e96084, <https://doi.org/10.1371/journal.pone.0096084>, 2014.

865 Rokach, L.: Decision forest: Twenty years of research, *Inform. Fusion.*, 27, 111-125,
866 <https://doi.org/10.1016/j.inffus.2015.06.005>, 2016.

867 Shakoor, A., Shakoor, S., Rehman, A., Ashraf, F., Abdullah, M., Shahzad, S. M., Farooq, T. H., Ashraf,
868 M., Manzoor, M. A., Altaf, M. M., and Altaf, M. A.: Effect of animal manure, crop type, climate
869 zone, and soil attributes on greenhouse gas emissions from agricultural soils-A global meta-analysis,
870 *J. Clean. Prod.*, 278, 124019, <https://doi.org/10.1016/j.jclepro.2020.124019>, 2021.

871 Sun, J., Liu, M., Fu, B. J., Kemp, D., Zhao, W. W., Liu, G. H., Han, G. D., Wilkes, A., Lu, X. Y., Chen,
872 Y. C., Cheng, G. W., Zhou, T. C., Hou, G., Zhan, T. Y., Peng, F., Shang, H., Xu, M., Shi, P. L., He, Y.
873 T., Li, M., Wang, J. N., Tsunekawa, A., Zhou, H. K., Liu, Y., Li, Y. R., and Liu, S. L.: Reconsidering
874 the efficiency of grazing exclusion using fences on the Tibetan Plateau, *Sci. Bull.*, 65, 1405-1414,
875 <https://doi.org/10.1016/j.scib.2020.04.035>, 2020.

876 Sun, Y. X., Liu, S. L., Liu, Y. X., Dong, Y. H., Li, M. Q., An, Y., and Shi, F. N.: Grazing intensity and
877 human activity intensity data sets on the Qinghai - Tibetan Plateau during 1990 - 2015, *Geoscience.*
878 *Data. Journal.*, 9, 140-153, <https://doi.org/10.1002/gdj3.127>, 2021.

879 Tabassum, A., Abbasi, T., and Abbasi, S. A.: Reducing the global environmental impact of livestock
880 production: the minilivestock option, *J. Clean. Prod.*, 112, 1754-1766,

881 <https://doi.org/10.1016/j.jclepro.2015.02.094>, 2016.

882 Van Boeckel, T. P., Prosser, D., Franceschini, G., Biradar, C., Wint, W., Robinson, T., and Gilbert, M.:
883 Modelling the distribution of domestic ducks in Monsoon Asia, *Agr. Ecosyst. Environ.*, 141, 373-380,
884 <https://doi.org/10.1016/j.agee.2011.04.013>, 2011.

885 Veldhuis, M. P., Ritchie, M. E., Ogotu, J. O., Morrison, T. A., Beale, C. M., Estes, A. B., Mwakilema,
886 W., Ojwang, G. O., Parr, C. L., Probert, J., Wargute, P. W., Hopcraft, J. G. C., and Han, O.:
887 Cross-boundary human impacts compromise the Serengeti-Mara ecosystem, *Science.*, 363,
888 1424-1428, <https://doi.org/10.1126/science.aav0564>, 2019.

889 Venglovsky, J., Sasakova, N., and Placha, I.: Pathogens and antibiotic residues in animal manures and
890 hygienic and ecological risks related to subsequent land application, *Bioresour. Technol.*, 100,
891 5386-5391, <https://doi.org/10.1016/j.biortech.2009.03.068>, 2009.

892 Waha, K., van Wijk, M. T., Fritz, S., See, L., Thornton, P. K., Wichern, J., and Herrero, M.: Agricultural
893 diversification as an important strategy for achieving food security in Africa, *Glob. Chang. Biol.*, 24,
894 3390-3400, <https://doi.org/10.1111/gcb.14158>, 2018.

895 Wang, R. J., Feng, Q. S., Jin, Z. R., and Liang, T. G.: The Restoration Potential of the Grasslands on the
896 Tibetan Plateau, *Remote. Sens.*, 14, 80, <https://doi.org/10.3390/rs14010080>, 2021.

897 Wang, Y. F., Lv, W. W., Xue, K., Wang, S. P., Zhang, L. R., Hu, R. H., Zeng, H., Xu, X. L., Li, Y. M.,
898 Jiang, L. L., Hao, Y. B., Du, J. Q., Sun, J. P., Dorji, T., Piao, S. L., Wang, C. H., Luo, C. Y., Zhang, Z.
899 H., Chang, X. F., Zhang, M. M., Hu, Y. G., Wu, T. H., Wang, J. Z., Li, B. W., Liu, P. P., Zhou, Y.,
900 Wang, A., Dong, S. K., Zhang, X. Z., Gao, Q. Z., Zhou, H. K., Shen, M. G., Wilkes, A., Mieke, G.,
901 Zhao, X. Q., and Niu, H. S.: Grassland changes and adaptive management on the Qinghai-Tibetan
902 Plateau, *Nat. Rev. Earth. Env.*, 3, 668-683, <https://doi.org/10.1038/s43017-022-00330-8>, 2022.

903 Wang, Y. X., Sun, Y., Wang, Z. F., Chang, S. H., and Hou, F. J.: Grazing management options for
904 restoration of alpine grasslands on the Qinghai - Tibet Plateau, *Ecosphere.*, 9, e02515,
905 <https://doi.org/10.1002/ecs2.2515>, 2018.

906 Wei, Y. Q., Lu, H. Y., Wang, J. N., Wang, X. F., and Sun, J.: Dual Influence of Climate Change and
907 Anthropogenic Activities on the Spatiotemporal Vegetation Dynamics Over the Qinghai-Tibetan
908 Plateau From 1981 to 2015, *Earth's Future.*, 10, 1-23, <https://doi.org/10.1029/2021EF002566>, 2022.

909 Yang, J. and Huang, X.: The 30 m annual land cover dataset and its dynamics in China from 1990 to
910 2019, *Earth. Syst. Sci. Data.*, 13, 3907-3925, <https://doi.org/10.5194/essd-13-3907-2021>, 2021.

911 Yang, Y. J., Song, G., and Lu, S.: Assessment of land ecosystem health with Monte Carlo simulation: A
912 case study in Qiqihaer, China, *J. Clean. Prod.*, 250, 119522, 2020.

913 Ye, T., Liu, W. H., Mu, Q. Y., Zong, S., Li, Y. J., and Shi, P. J.: Quantifying livestock vulnerability to
914 snow disasters in the Tibetan Plateau: Comparing different modeling techniques for prediction,
915 *International Journal of Disaster Risk Reduction*, 48, <https://doi.org/10.1016/j.ijdrr.2020.101578>,
916 2020.

917 Zhai, D. C., Gao, X. Z., Li, B. L., Yuan, Y. C., Jiang, Y. H., Liu, Y., Li, Y., Li, R., Liu, W., and Xu, J.:
918 Driving Climatic Factors at Critical Plant Developmental Stages for Qinghai-Tibet Plateau Alpine
919 Grassland Productivity, *Remote. Sens.*, 14, 1564, <https://doi.org/10.3390/rs14071564>, 2022.

920 Zhan, N., Liu, W. H., Ye, T., Li, H. D., Chen, S., and Ma, H.: High-resolution livestock seasonal
921 distribution data on the Qinghai-Tibet Plateau in 2020, *Sci. Data.*, 10, 142,
922 <https://doi.org/10.1038/s41597-023-02050-0>, 2023.

923 Zhang, B. H., Zhang, Y. L., Wang, Z. F., Ding, M. J., Liu, L. S., Li, L. H., Li, S. C., Liu, Q. H., Paudel,
924 B., and Zhang, H. M.: Factors Driving Changes in Vegetation in Mt. Qomolangma (Everest):

925 Implications for the Management of Protected Areas, *Remote. Sens.*, 13, 4725,
926 <https://doi.org/10.3390/rs13224725>, 2021a.

927 Zhang, R. Y., Wang, Z. W., Han, G. D., Schellenberg, M. P., Wu, Q., and Gu, C.: Grazing induced
928 changes in plant diversity is a critical factor controlling grassland productivity in the Desert Steppe,
929 Northern China, *Agr. Ecosyst. Environ.*, 265, 73-83, <https://doi.org/10.1016/j.ageec.2018.05.014>,
930 2018.

931 Zhang, W. B., Li, J., Struik, P. C., Jin, K., Ji, B. M., Jiang, S. Y., Zhang, Y., Li, Y. H., Yang, X. J., and
932 Wang, Z.: Recovery through proper grazing exclusion promotes the carbon cycle and increases
933 carbon sequestration in semiarid steppe, *Sci. Total. Environ.*, 892, 164423,
934 <https://doi.org/10.1016/j.scitotenv.2023.164423>, 2023.

935 Zhang, Y., Hu, Q. W., and Zou, F. L.: Spatio-Temporal Changes of Vegetation Net Primary Productivity
936 and Its Driving Factors on the Qinghai-Tibetan Plateau from 2001 to 2017, *Remote. Sens.*, 13, 1566,
937 <https://doi.org/10.3390/rs13081566>, 2021b.

938 Zhao, X. Q., Xu, T. W., Ellis, J., He, F. Q., Hu, L. Y., and Li, Q.: Rewilding the wildlife in
939 Sangjiangyuan National Park, Qinghai-Tibetan Plateau, *Ecosyst. Health. Sust.*, 6, 1776643,
940 <https://doi.org/10.1080/20964129.2020.1776643>, 2020.

941 Zhou, W. X., Li, C. J., Wang, S., Ren, Z. B., and Stringer, L. C.: Effects of grazing and enclosure
942 management on soil physical and chemical properties vary with aridity in China's drylands, *Sci.*
943 *Total. Environ.*, 877, 162946, <https://doi.org/10.1016/j.scitotenv.2023.162946>, 2023.

944 Zhu, Q., Chen, H., Peng, C. H., Liu, J. X., Piao, S., He, J. S., Wang, S. P., Zhao, X. Q., Zhang, J., Fang,
945 X. Q., Jin, J. X., Yang, Q. E., Ren, L. L., and Wang, Y. F.: An early warning signal for grassland
946 degradation on the Qinghai-Tibetan Plateau, *Nat. Commun.*, 14, 6406,
947 <https://doi.org/10.1038/s41467-023-42099-4>, 2023a.

948 Zhu, Y. Y., Zhang, H. M., Ding, M. J., Li, L. H., and Zhang, Y. L.: The Multiple Perspective Response
949 of Vegetation to Drought on the Qinghai-Tibetan Plateau, *Remote. Sens.*, 15, 902,
950 <https://doi.org/10.3390/rs15040902>, 2023b.

951 Zhou, J., Niu, J., Wu, N., Lu, T. Annual high-resolution grazing intensity maps on the Qinghai-Tibet
952 Plateau from 1990 to 2020 [Dataset]. Zenodo.
953 <https://doi.org/10.5281/zenodo.1085111913672152141090>, 2024.

域代码已更改